TECHNICAL REVIEW

No.17 / March 2022

Technical Review
MAPNA TURBINE ENGINEERING & MANUFACTURING CO. (TUGA)

TUGA
MAPNA GROUP

Willpower to Empower Generations

TECHNICAL REVIEW

Cover Page:
A MAPNA Turbine technician standing in front of an MGT-70 assembly platform

Editorial

Dear Colleagues, Partners and Professionals,

At MAPNA Turbine we are constantly learning, adapting and evolving to help our clients by delivering world-class solutions with beneficial impacts on their bottom lines. A brief account of a few recent technological achievements is presented to you, our valued readers, in this edition of MAPNA Turbine Technical Review.

The first article takes an in-depth look into the design of MST-40C as the first three-level-pressure steam turbine designed by MAPNA Turbine engineers to be mated with our new MGT-75 gas turbine product in the near future to deliver 59.5% efficient combined cycle. It spells out in detail all meticulous steps taken to design different parts and components of the machine including but not limited to the last stage blades, the steam path, the rotor and casings as well as all the related auxiliary systems.

The second article takes a sneak peek into the latest upgrade scheme already laid out and pursued at MAPNA Turbine for our flagship MGT-70 gas turbine. One of the key attributes of the new upgrade scheme is, among others, the extension of the current periodic inspection intervals of 33,000 EOH to an incredibly high 50,000 EOH, equivalent to almost 6 years of normal operation. Therefore, significant operating and maintenance cost reductions and fewer power plant outages would be expected, to the full benefit of our clients.

Steps taken to improve MGT-40 gas turbine output at some ambient conditions via compressor blades' stagger angles are elaborated on in the third article. This would be beneficial for some customers of the machine. A number of analysis and optimization tools, including an internally developed cycle analysis code, have been taken advantage of in the new design to reduce the associated computational time and costs to a significant extent.

The fourth article features a thorough investigation into the effects of different scanning strategies and support geometries and dispositions on subsequent residual stress and distortion of Inconel 625 SLM additively manufactured parts. The results of the combined experimental–computational analyses shed more light on the complex nature of the process and allow for more precise and reliable outcomes.

The last article reflects on two of the latest improvements made to make final assembly process of MGT-70 gas turbines more efficient and less time consuming. This was achieved by ruling out and optimization of the prolonged processes of using dummy shafts for the casing/bearing alignments and the two-step rotor blades grinding.

Please join us in relishing a detailed account of these subjects in this issue of the Technical Review.

Respectfully,

Mohammad Owliya, PhD

Managing Director

MAPNA Turbine Company (TUGA)

March 2022

Contents

1

An In-depth Look at MST-40C Steam Turbine Design

Modarres, Ali

MAPNA Turbine Engineering & Manufacturing Co. (TUGA)

Introduction

MAPNA Turbine has started manufacturing a brand new gas turbine branded as MGT-75 with nominal power output of 220 MW and 217 MW in simple and combined cycle applications respectively. This machine falls into F-Class category with TIT (Turbine Inlet Temperature) of 1230 °C and TET (Turbine Exit Temperature) of 578 °C. MGT-75 was domestically designed by MAPNA Turbine engineers, ideally suiting relatively low budget projects, taking into account its relatively lower power in comparison with other major OEMs' products of the same class, while maintaining the efficiency at a world-class level.

In order to better exploit the heat of the exhaust gas of the newly designed gas turbine, it was decided to design a 3-level-pressure steam turbine designated as MST-40C. The condensing steam turbine produces 102 MW with reheat steam flow, meant to increase the combined cycle efficiency to 59.5% at standard ISO conditions.

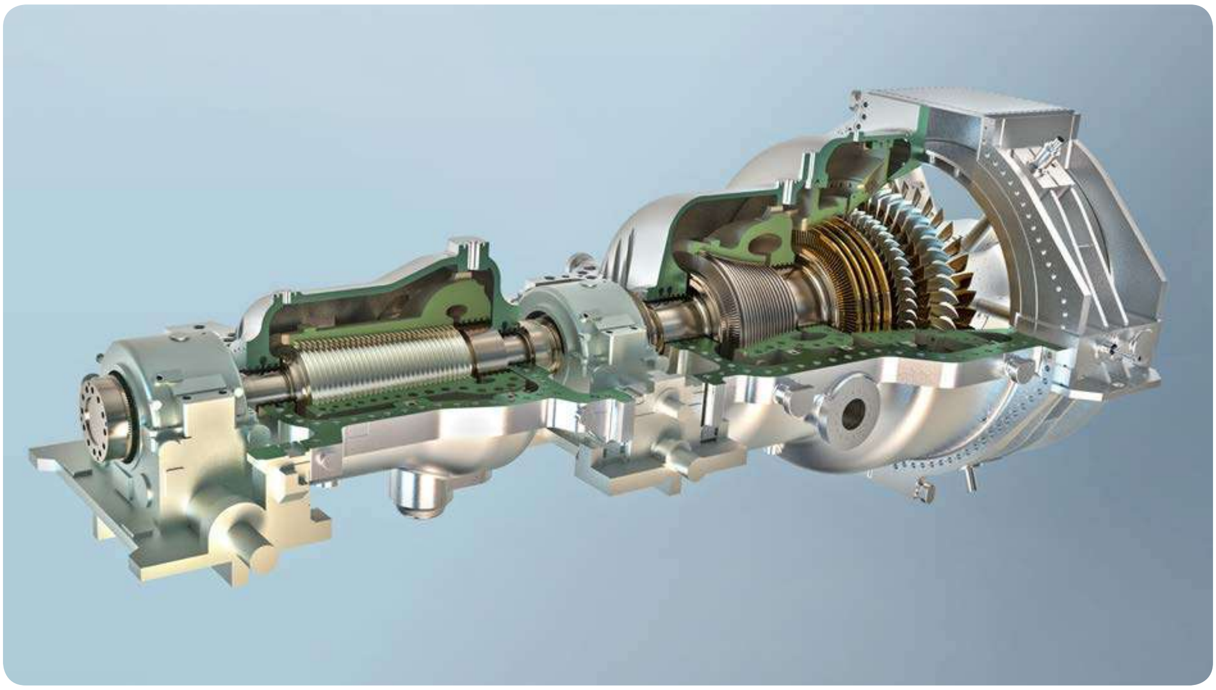

Fig. 1 – MST-40C steam turbine 3-D model

The last stage blades of this machine have been designed and sized to have the best possible performance in typical domestic sites with relatively high condenser pressures. Moreover, MAPNA Turbine's in-house technology has been utilized for designing upstream stages, as well as rotor features and casings.

Design Features

■ Steam Stream

Steam first enters the HP section at a temperature of 565 °C and exits the section as CRH (Cold Re-Heat) stream, flowing back to the HRSG to become heated up again to the main steam temperature. The HRSG's second pressure steam (IP) mixes with the CRH steam right before reheating. The HRH (Hot Re-Heat) steam enters the IP section at the middle of the IP outer casing and at the same temperature of 565 °C where it passes through the section blading. The HRSG's third pressure steam (LP) then blends with the IP outlet steam within the IP outer casing area, flowing to the LP section. The exhaust steam eventually flows on to the condenser. There are 31, 16 and 6 stages in the HP, IP, and LP sections respectively.

To find a balance between the equipment price and cycle efficiency, it is economical to use three-level-pressure steam turbines for F-Class gas turbines meaning that the HRSG would produce steam at three different pressure levels (115 bar, 26 bar and 5 bar for instance). This ensures that water absorbs as much energy as possible from the gas turbine exhaust, while keeping the equipment price at a reasonable level. Although having more pressure levels would slightly increase the overall efficiency, it is not an economically viable option.

■ Key Points Considered

There are a number of key points that had to be considered while designing the machine. First of all, the turbine had to be compatible with ACC (Air-Cooled Condenser) system. This is because Heller type condensers have been crossed off MAPNA Group's standard cooling system options and are only used on client's request and unless the plant is near the sea or a big river allowing for application of once-through cooling systems, ACC cooling systems are the only viable option for newly built plants or those that are about to be launched.

Secondly, attempt was made to keep the resultant thrust force at the minimum permissible value. This has been achieved by selecting the steam path configuration, so that the HP and IP sections face the generator, whereas the LP section is in the reverse direction towards the condenser. As a result, there is no need for huge thrust bearings to counter large thrust forces. Thanks to this configuration, impermissible temperature difference between the upper and lower halves of the IP outer casing is ruled out as well, as it does not let the steam get trapped between the IP inner and outer casings. When steam does get trapped in there, hotter steam might be collected within the upper half and less hot steam within the lower half resulted from a weak ventilation caused by low LP steam inlet flow. In the current configuration, there is always enough steam flow between the IP inner and outer casings, giving rise to strong ventilation and blending in that area.

Thirdly, the IP-LP rotor had to comprise three parts welded together. This is mainly because the material has to be able to withstand high thermal stresses or high centrifugal forces wherever required. Since the IP steam enters at the middle of the outer casing, the part in the middle has to be resistant to high steam temperatures. The other two parts however, experience high centrifugal forces and stresses. Moreover, the welding feature gives the designer more freedom to choose higher steam temperatures compared to the case when the entire rotor is made of a single part. Welded rotor also gives the designer another advantage: Manufacturing on a modular design basis. Unlike gas turbines, steam turbines are normally subject to customization and change of the LP end, based on site conditions. The more volumetric flow at the exhaust because of low condenser pressure, the larger the exhaust annulus area. This should be noted that each last stage blade set has its own setup of tip and hub diameters, axial chord, clearances, etc., so it is not simply replaceable. Therefore if a larger LP end is to be used, the rotor will have to be thicker. Thanks to the welding feature of the rotor, the LP end is able to be selected and customized individually while keeping the upstream stages unchanged.

■ Steam Parameters

Steam parameters, i.e., pressure, temperature and flow rate were finalized in a mutual information exchange within MAPNA Group, so that all parties involved in designing the steam cycle came to a consensus. The rather high condenser pressure was particularly chosen in a way that the turbine would be compatible with typical Iranian site conditions. As a result, the last stage blade set was designed. The key issue was calculating the exhaust annulus area so that the exiting flow velocity would be about 240 m/s which is quite normal for a steam turbine LP end.

The agreed upon steam parameters are listed in Table 1.

Table 1 – MST-40C steam parameters

Item	Parameter	Value	Unit
1	Main steam flow rate	60.8	kg/s
2	Main steam temperature	565	°C
3	Main steam pressure	112.6	bar
4	Reheat steam flow rate	68.3	kg/s
5	Reheat steam temperature	565	°C
6	Reheat steam pressure	26.6	bar
7	LP steam flow rate	6.7	kg/s
8	LP steam temperature	233	°C
9	LP steam pressure	3.7	bar
10	Condenser pressure	0.082	bar
11	Power output	102	MW

■ Last Stage Blades Design

As mentioned earlier, the last stage sizing was carried out so as to have a good performance at high condenser pressures, keeping an eye on normal operating conditions with low back pressures. The exhaust velocity of 240 m/s was selected on account of the ACC cooling system type. Among different cooling systems, ACC has rather large pressure fluctuations, particularly when the turbine is in the startup phase. Therefore an LP end sized to cope with high back pressures, and still providing an acceptable performance in low back pressure conditions would be of great benefit. The hub diameter of the upstream stages depended on the sizing of the LP end.

The second issue following setting the exhaust annulus area was the layout of the LP end stages. There are various types of LP last stage rotary blades, e.g., free-standing, snubber type, integrally shrouded, and combinations of the above. For MST-40C, bearing in mind that the last blades were the first set of the kind to be designed, free-standing type was selected which is easier to design and also simpler to assemble/disassemble. However, significant tip leakage associated with this type of layout, could be a drawback.

The material of the blades was selected on the basis of water droplet erosion index. This index is calculated taking into account the linear blade velocity, the steam quality at the exhaust, the turbine speed and other parameters. This very index determines which of the two blade hardening methods (flame or laser hardening) shall be used. For the designed 3.7 m^2 set of LP end blades (TF-37) particularly, flame hardening method was chosen to be used.

Fig. 2 – TF-37; Last stage blade set designed for MST-40C steam turbine

Considering the fact that typical Iranian sites have rather high condenser pressures, it was deemed necessary to design the LP blades capable of withstanding such operational conditions that happen mostly in the summertime. The higher the allowable condenser pressure, the better and more economical the cooling system performance. For this reason, 0.5 bar was targeted as the relevant trip value. This should be noted that the designed set of LP blades is applicable to a range of turbine power outputs. Roughly speaking, TF-37 may be used in turbines with outputs from 70 MW up to 120 MW. Thanks to rotor welding feature, it is possible to manufacture the IP-LP rotor on a modular design basis. In other words, this rotor is able to be customized for different condenser pressures.

■ Steam Path Design

The first step following the design/selection of the LP end, was calculating the number of stages for each section. The curve of efficiency against velocity ratio, i.e. the ratio of linear blade velocity over equivalent velocity of isentropic enthalpy drop across the stage, has a dome shape for each section. The dome indicates that both too low and too high velocity ratios would result in stage efficiency drop. Having too few stages means high enthalpy drop and thus low velocity ratio, whereas too many stages would mean the opposite. Therefore the number of stages shall be meticulously calculated to bring about the best possible efficiency for each section of blades. As mentioned earlier, 31, 16 and 6 stages were calculated for HP, IP and LP sections, respectively.

Aside from the above, there are various configurations of the steam path each with their own pros and cons. For instance, HP and IP sections may be on a single rotor in a separate cylinder and LP in another one, or HP section in one cylinder and IP and LP sections in another. In addition, each section can face either the generator or the condenser. For each option, the direction of the thrust force applied on the blades by the steam flow must be taken into account. This is because the resultant force on the entire rotor train shall not be more than a pre-assumed limit regardless of the number of rotors. This becomes important when it comes to thrust bearing design. If the bearing was to withstand too much of thrust forces, it would need to be bulky, resulting in huge oil consumption in the lube oil system design. Moreover, the rotor collar meant to face thrust pads would also need to be too large.

The profile used for drum blades was our in-house technology which not only provided acceptable efficiency but also was more familiar to our manufacturing department staff translating into easier production processes and fewer non-conformities involved. This profile was made use of throughout the turbine steam path, with different stagger angles, heights, and scales though.

The hub slope angle of steam path is usually a multiplication of 1.5 degrees and may be selected based on the designer's preferences. This parameter affects the hub-to-tip ratio of each blade row. Lower values mean longer blades and thinner rotors and vice versa. As the linear velocities of the blade hub and tip get close to each other, they do not require twisted airfoil. This is because the added efficiency of the twisting feature is not worth the manufacturing difficulty of the airfoil. However, thicker rotor resulted from high hub-to-tip ratio of the blades brings about heavier components, bigger bearings, more oil consumption and higher price. On the other hand, lower values of hub-to-tip ratio (say 0.75) lead to longer blades which may need twisting. In addition to difficult manufacturing, special provisions are needed for roots of the blades on which higher centrifugal force is applied. A compromise is inevitable considering all of the above mentioned mechanical, aerodynamic, economical and manufacturing aspects. Attempt was made to design cylindrical type HP and IP stages, allocate twisted blades to the LP section only, and keep the rotor diameter in the common practice range for a typical 100 MW turbine.

The main steam enters the HP section through one set of HP stop and control valves. In a similar way, the reheat steam has one set of IP stop and control valves integrated into a common casing. The LP steam has its own stop and control butterfly valves. The position of the HP and IP valves relative to the casing, whether left or right, was meticulously selected in order to avoid steam turbulence when reaching the leading edges of the first row. Bearing in mind that the valves have been positioned sideways, the steam flows in a circular motion downstream the valves. This means that the incidence angle at the first stage may be biased either to positive or negative relative to 0°. The latter has a worse impact like braking against the blade. So, the valves' position has been chosen to avoid such detrimental consequences by establishing positive incidence angles.

Two types of sealing including labyrinth and tip-to-tip were considered in this machine. The labyrinth seals have better function and less leakage; however, since this type of sealing has limited relative axial expansion, they can only be used for portions close to the thrust bearing. For the regions such as the LP section that are away from the axial fixed points, tip-to-tip seals were applied. Proper function of the seals in both hot and cold working conditions was thoroughly investigated.

■ Rotor Design

Following the steam path design, the rotors were designed so as to allow for higher steam temperatures at the inlet while having higher strength against centrifugal stresses wherever required, fewer bearings needed and also offer a modular manufacturing scheme.

It was deemed necessary at the beginning of the project to consider exhausts with different annulus areas for different site conditions. However the change in the LP end should not give rise to a new IP-LP rotor design. This can expedite the procurement and manufacturing of the rotor for mass production. In other words, the IP-LP rotor was designed with three parts welded together with two welding seams. The middle part and the IP section can be procured on a "make-to-stock" basis, whereas the LP portion is supplied as per each specific order in a "make-to-order" fashion.

Fewer bearings is considered a substantial benefit which was taken advantage of in the design of this machine. The weight of the HP rotor, shown in Fig. 3, is borne by two bearings, a journal as well as a combined journal-thrust bearing. The IP-LP rotor however has only got one bearing located at the LP exhaust section. The other end of this rotor is coupled to the HP rotor and its weight is borne by a common combined journal-thrust bearing. The details of stiffness and damping coefficients have been finalized with a bearing supplier and fine-tuned to not allow the natural lateral and torsional frequencies to fall within the impermissible ranges.

Fig. 3 – 3-D model of the MST-40C HP rotor

Choosing the thrust bearing to be located between the HP and IP-LP sections brings about the advantage of moderate axial expansions to the possible extent for different areas of the rotors/casings including the most extreme ends. The advantage lies in the selection of the sealing type, so that labyrinth seals could be used for more areas compared to the case with large axial expansions. This would provide far less steam leakages, leading to a higher overall efficiency.

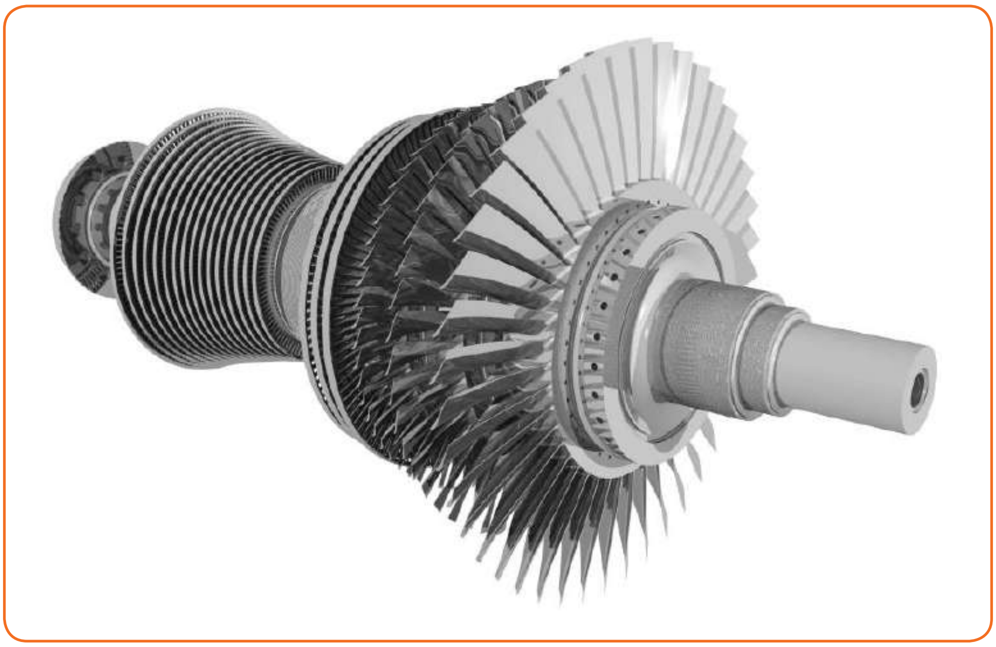

Fig. 4 – 3-D model of the MST-40C IP-LP rotor

Care was also taken to spare the operators the difficulties typically associated with balancing of the rotor on site by designing an opening on the outer casing's upper half precisely aligned with the rotor's balancing bolts.

A hydro-motor was located at the very end of the rotor train behind the generator, as the turning gear to rotate the rotor at 60 rpm during startup and shutdown operations. The motor is fed by the oil coming from the main lube oil system. A clutch is also considered to disconnect the motor from the rotor train when the train rotating speed reaches 600 rpm.

■ Casing Design

Steam inlets at both HP and IP-LP sections are located in lower halves, so that the operator does not need to cut/decouple the inlet pipes to open the upper halves. This would be most beneficial during maintenance operations and the turbine can get back to operation more quickly.

The openings allocated for fastening balancing bolts can also be used for both borescope inspections as well as air dryer connections that come in handy in safe long-term preservation of the machine.

Both HP and IP-LP outer casings are constrained in three directions within the combined journal-thrust bearing pedestal, so that they cannot move in any direction at this point. The LP exhaust casing is fixed laterally and vertically, and can only expand axially. An expansion joint provided in the cooling system prevents this axial expansion from being transmitted to the condenser. Similar to the outer casings, the inner casings, i.e. HP and IP inner casings are fixed at one end and can move at the other within the outer casings.

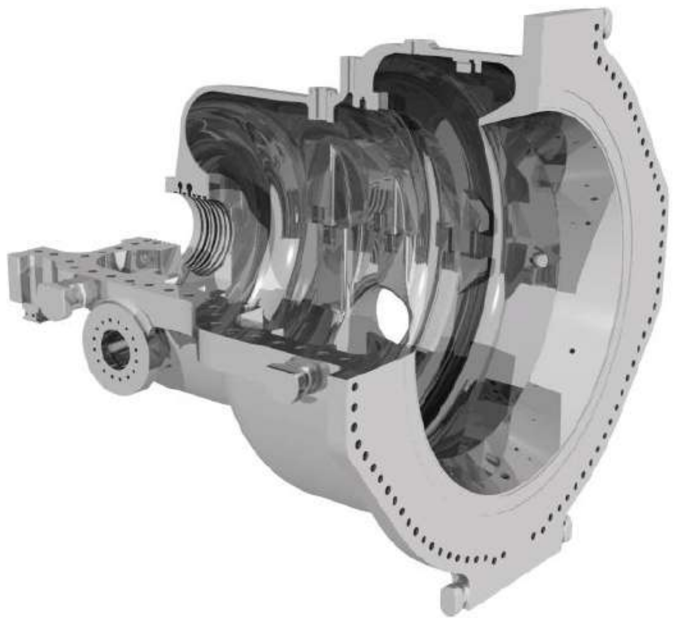

Fig. 5 – 3-D model of the MST-40C IP-LP outer casing

Casings' thicknesses are calculated based on steam pressure at each specific compartment. The HP inner casing is the thickest and LP stationary blade rings are the thinnest of all parts.

There are thermocouple insertion points considered on the HP and IP inner casings to allow for inner surface temperature readings. These values are assumed equal to the rotor surface temperature at those points.

Knowing the rotor surface temperature in addition to the steam mass flow rate and temperature, the temperature gradient across the rotor section could be calculated. This input is required to provide startup and shutdown curves for the machine.

Water drainage nozzles have been placed within the outer casings wherever needed. The nozzles are welded onto an inter-connected piping which in turn is routed down to the flash pipe through drain valves. The valves are open when the turbine is in cold condition and is starting up. In this phase a mixture of steam and condensate is drained off to ensure no condensate is accumulated in the lower half of the outer casings. If this does not happen for any reason, the machine would experience an oval-shape distortion giving rise to blade tips clearance reduction which might lead to seal rubbing in extreme circumstances.

■ Auxiliary Systems

MST-40C steam turbine has a set of auxiliary systems arranged round the turbo-generator set, as follows:

- Sealing system (seal steam, leak off, gland steam condenser)
- Lube oil system (lube oil module, clean and dirty oil tanks, oil purifier)
- Control fluid system
- Drainage system
- Bypass system (IP and LP bypass stations)
- Condensation system (hood spray, flash pipe spray, bypass station spray, etc.)
- Control air

The sealing system ensures that there is no air ingress and no steam leakages into the atmosphere during turbine operation.

The lube oil system feeds the turbine and generator bearings with lubricating and lifting oils at two different pressures. The lifting oil system lifts the rotor train by 0.1 mm to make sure that no metal-to-metal contact is happening. This system is kept in service until the train speed exceeds 600 rpm.

The control fluid system provides hydraulic oil for electro-hydraulic actuators. The consumers include HP, IP and LP steam stop, control and bypass valves. Although the HP bypass valve is out of MAPNA Turbine's scope of supply, its required hydraulic oil is provided by the turbine's control fluid system.

The drainage system is meant to ensure that there is no condensate accumulation within the valves and casings. The drain valves are of fail-to-open type to make sure that in case of any malfunction in the control air system, the drainage system operates properly. The drain valve actuators are of pneumatic type and provided with control air supplied by an air compressor.

Bypass valves allow for the passage of the steam coming from the HRSG to the condenser whenever not needed by the machine. They are mainly used during turbine startups and load rejection modes. At startups, part of steam is admitted to the turbine and the rest flows to the condenser via the IP and LP bypass valves. In a similar way, the unwanted portion of the HP steam bypasses the turbine and flows to the CRH pipe. At the design load, the bypass valves are fully closed.

The condensation system includes water sprays wherever required, e.g. downstream of bypass valves, downstream of the last moving blade row of the LP section and the flash pipe. The purpose is to cool down the hot steam to avoid heating and harming the bearings or condenser. In case of very low steam flow (in load rejection, for instance), steam is circulated back and forth within the LP end stages causing a temperature rise in that area. This gives rise to the heating of the LP bearing, leading to non-uniform bearing distortion. As a consequence, blade tip clearances might be altered which could end up in rubbing in extreme cases.

Concluding Remarks

MST-40C is a three-level-pressure machine designed by MAPNA Turbine. The machine was designed in close coordination and data exchange with other MAPNA Group companies. Various LP ends, improved steam parameters and improved auxiliary systems are as among potential product upgrades in the future.

2

MGT-70(4); A Sneak Peek into the Latest MGT-70 Gas Turbine Upgrade Scheme

Faghfoor, Saeed
Poursamad, Amir
Hashemi, Omidreza

MAPNA Turbine Engineering & Manufacturing Co. (TUGA)

Introduction

MAPNA Turbine have unveiled their ambitions to introduce a new upgrade for MGT-70 gas turbine platform entitled 'MGT-70(4)' soon. The main goal of this new upgrade scheme is to achieve enhanced lifecycle for gas turbine hot components along with higher power generation and thermal efficiency. The Turbine Inlet Temperature (TIT) will be increased to achieve outstanding 190 MW power output mark, which makes it necessary to reanalyze cooling schemes of gas turbine vanes and blades and to introduce some design modifications to cope with the new TIT.

Operating MGT-70 Gas Turbine Fleet

There are a number of criteria by which a successful gas turbine upgrade is judged, including performance, availability, starting reliability, equipment lifecycle and operational flexibility. Considering current competitive environment, improvement in any of the above-mentioned areas could lead to product adoption in the market. Following this approach and providing the operators with beneficial upgrades and improvements, MGT-70 gas turbine has achieved a remarkable success in the market in recent years.

To date, three upgraded versions of the machine have been introduced to the market, besides several other improvement packages such as a series of MGTboost-70 platform, IGV+, Wet Compression and MAPTune-70 to name a few.

Evolution of MGT-70 gas turbine product since its initial version in 2002 by MAPNA Turbine is shown in Fig. 1. The last upgraded version of MGT-70 gas turbine product, i.e., MGT-70(3), was introduced in 2017. Thus far, more than 15 new units have been delivered to the customers and more than 14 older units have been upgraded to this version in Iran and abroad. In about 4 years of operation, the fleet has amassed more than 260,000 operating hours demonstrating remarkable availability and run/start reliability.

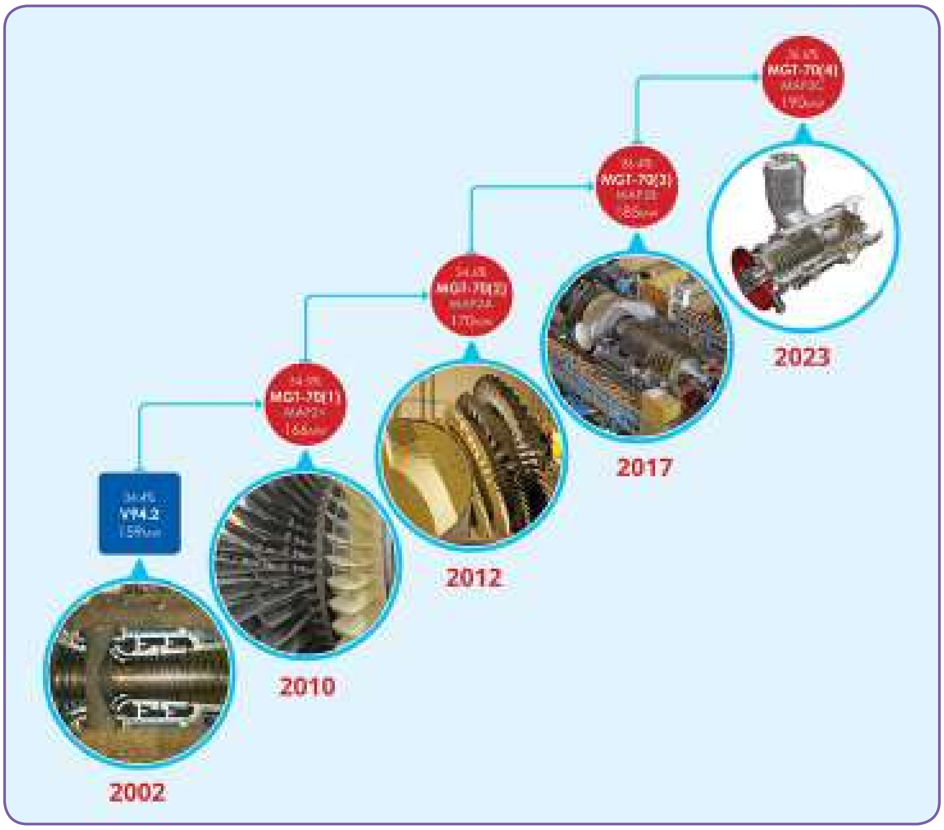

Fig. 1 – MGT-70 gas turbine evolution

MGT-70(4) Upgrade Scheme

Following successful previous product upgrades for MGT-70 gas turbine, the new MGT-70(4) upgrade scheme has been planned taking into account the following considerations:

The new upgrade scheme is aimed at providing the customers with the minimum operational costs possible whilst increasing the performance parameters and extending the unit lifecycle as much as physically practicable.

The main focus of the new upgrade scheme would be to extend the present inspection intervals, i.e. 33000 EOH (about 4 years of normal operation) to a new outstanding value of 50,000 EOH (about 6 years of normal operation) for a power generation gas turbine unit. To achieve this ambitious goal, a comprehensive study on mechanical conditions of hot gas path components in addition to a defect survey on components during operation was conducted. New gas turbine inspection interval was suggested to reduce the outage period of the unit required for inspection and refurbishment of parts, leading to improved availability of the gas turbine. Meanwhile, total costs associated with overhaul inspections during gas turbine lifecycle will also be reduced.

The new upgrade scheme will bring about improved performance parameters to the highest values attainable by E-class gas turbines as a result of modifications implemented on gas turbine vanes and blades cooling scheme allowing for an increased TIT to an unprecedented value of 1105 °C. Consequently, several hot gas path parts and components will also be modified to better withstand the higher operating temperatures at these sections of the machine.

While former upgrades sometimes warranted fundamental changes in the plant, this one can be carried out for in-service units through minor alterations and hence reduction in time and money spent on the process. Although there were several upgrade scenarios to improve the performance of different components, some of them did not contribute to the intended goal of reaching 50,000 EOH limit and hence were ignored.

As a result of design enhancements and modifications made, the upgraded MGT-70(4) gas turbine will boast increases of up to 31 MW in power, and 2.2% in efficiency with respect to the original V94.2(3) gas turbine product in simple cycle applications.

Performance parameters of the last two upgraded versions of MGT-70 gas turbine product are listed in Table 1.

Table 1 – Performance parameters for MGT-70(3) & MGT-70(4) gas turbines

Product	Power Output [MW]	Efficiency [%]
MGT-70 (3)	185	36.4
MGT-70 (4)	190	36.6

Considering design modifications and preparation of related manufacturing prerequisites and procedures, the new upgraded product is expected to be launched by mid-2023.

■ Mechanical Design Improvements

Due to mechanical power increase at the end of driving shaft, there were concerns about the rotor integrity and attachments. Increasing TIT would also affect hot gas path components within combustion chamber, as well as vanes and blades of the turbine section. These components have been studied for strength and lifetime considerations.

In MGT-70 gas turbine platform and to integrate rotor parts, all shafts and disks are stacked together via Hirth-serration couplings and a central tie-rod and nut fastens all components to ensure a reliable rotor assembly. With the increase in the mechanical power output of the gas turbine, the strength and capacity of those couplings and connections of the turbine-generator coupling shaft needed to be checked. The power increase would also introduce some minor modifications in the rotor components. The effects of these changes were proved to be negligible and hence no concern about the shaft train’s dynamic behavior.

The aim of the study conducted on combustion chamber parts was to evaluate the strength as well as creep and fatigue life assessment. Related mechanical analyses were carried out based on temperature distributions obtained from the CFD analyses performed.

Although creep analysis is deemed to be the most important analysis in investigation of hot gas path parts and components, the stress analysis is a prerequisite for subsequent analyses. The results of stress analysis would be used to demonstrate critical points which may have high risks for initiation and development of any kind of damages such as fatigue crack or creep rupture initiation.

For life assessment procedure, creep behavior of components exposed to high temperature must be analyzed. Creep strain limits the life of combustion chamber components such as mixing chamber and hot gas casing and hence must be kept at a minimum. An innovative approach to take into account positive effects of compression stresses within a pressure vessel for creep life assessment of related parts and components was also developed. This scheme allows for more accurate creep life assessments to be performed in such huge shells.

- ### Gas Turbine Section Modifications

In redesigning the first stage vane of the MGT-70(4) gas turbine and despite the increased TIT, an attempt was made to reduce the maximum and bulk temperatures of the vane by making some improvements in the gas turbine blade cooling system. The sum of changes made to the cooling system resulted in 40 and 9 degrees of Celsius decrease in the maximum and bulk temperatures of the airfoil, respectively, while keeping the cooling air flow almost unchanged.

For the first stage blade of the MGT-70(4) gas turbine, the airfoil shape and serpentine cooling design of the MGT-70(3) were left unchanged. However, some modifications were made in the cooling system to reduce the bulk and maximum temperatures, to change the location of maximum temperature, and to keep both the blade life and coolant mass flow rate same as the baseline design despite the increased TIT. Thanks to these modifications, the maximum temperature decreased by about 10 K, and some major hot spots in the baseline design were also removed.

Modifications performed on the cooling system of the 2nd stage vanes of the MGT-70(4) gas turbine, have also led to reductions in critical lifetime parameters such as maximum and bulk temperatures as well as temperature gradients compared to the base design.

Concluding Remarks

After successful introduction of the last upgraded version of MGT-70 gas turbine product, i.e., MGT-70(3) in 2017, a new upgrade scheme is now planned and pursued at MAPNA Turbine to provide the customers with several outstanding benefits.

The new upgrade scheme is primarily aimed at extending the unit life cycle while improving the performance parameters of the machine. In this upgraded version, the TIT would be increased by 15 °C with respect to the previous version. To reach these goals, all major parts and components of the machine are assessed and analyzed to make sure that they can withstand the more severe working thermo-mechanical conditions they are going to be exposed to, considering the new extended maintenance intervals of the machine. As a result of the analyses performed, only the first stage vanes and blades in addition to the second stage vanes of the gas turbine would be redesigned and replaced in MGT-70(4) with respect to MGT-70(3) gas turbine product.

3

MGT-40 Gas Turbine Compressor Modification

Azizi, Rohollah
Ziamolki, Alireza
Nazari, Mohammad

MAPNA Turbine Engineering & Manufacturing Co. (TUGA)

Introduction

Gas turbines are generally designed for ISO standard conditions, and changes in ambient conditions such as temperature, pressure, and humidity substantially affect their performance; therefore, it is essential to provide solutions to prevent or diminish such unfavorable degradations. Temperature is the most critical ambient condition of all and an increase in this parameter leads to decreased air mass flow rate and hence a decrease in the power output and efficiency. It is estimated that, every 1 K increase in the ambient temperature from ISO conditions, leads to 0.5 to 0.9% drop in the power output [1] and 1% decrease in thermal efficiency of the machine [2].

In the present article, a method is presented to improve the performance of MGT-40 single shaft gas turbine at high ambient temperatures by changing the angle of compressor stator vanes. First, a three-dimensional simulation was carried out for the compressor compartment using a commercial CFD solver; afterwards, the gas turbine's performance was calculated using an in-house cycle analysis code. Next, design variables with the most significant impact on the power output were selected using the design of experiment (DoE) approach and finally, optimization was performed to find the optimum stagger angles. The optimization process is based on a genetic algorithm coupled with an artificial neural network.

Numerical Simulations

Performance of the MGT-40 gas turbine compressor comprising Inlet Guide Vanes (IGVs), 17 stages of rotary and stationery blades, as well as two rows of Exit Guide Vanes (EGVs), as shown in Fig. 1, was investigated in the present study using a 3-D finite volume CFD solver. Steady-state solution was used to solve the Reynolds-averaged Navier-Stokes (RANS) equations within the domain under investigation.

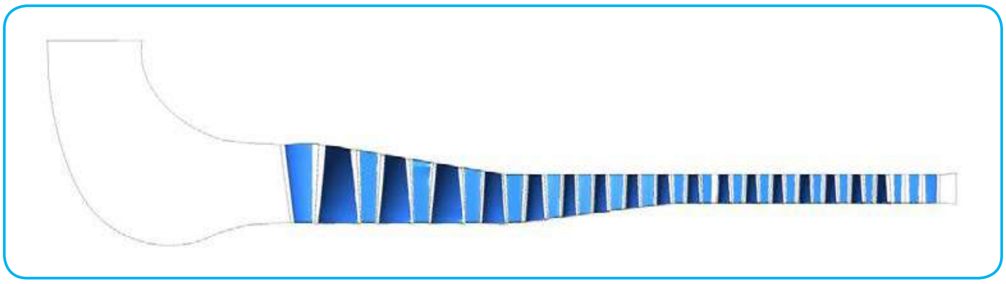

Fig. 1 – Meridional view of MGT-40 gas turbine axial compressor

Cycle Performance Analysis

The objective of this investigation was to enhance the performance of the MGT-40 gas turbine's cycle during hot seasons. Therefore, the effects of the compressor blades' re-staggering on the cycle performance had to be studied. Related thermodynamic simulations were performed using in-house software called MapCycle, previously developed for performance analysis of single and multi-shaft gas turbines.

MapCycle inputs include environmental conditions, axial speed, pressure drop at the compressor inlet, and inlet mass flow rate. It provides parameters such as temperature, pressure and mass flow rate at different gas turbine components, in addition to the characteristics of the compressor performance such as pressure ratio, efficiency, and corrected mass as outputs. A graphical representation of MapCycle's architecture indicating various inputs and outputs at different parts of the code corresponding to different parts and components of a turbogenerator set is shown in Fig. 2.

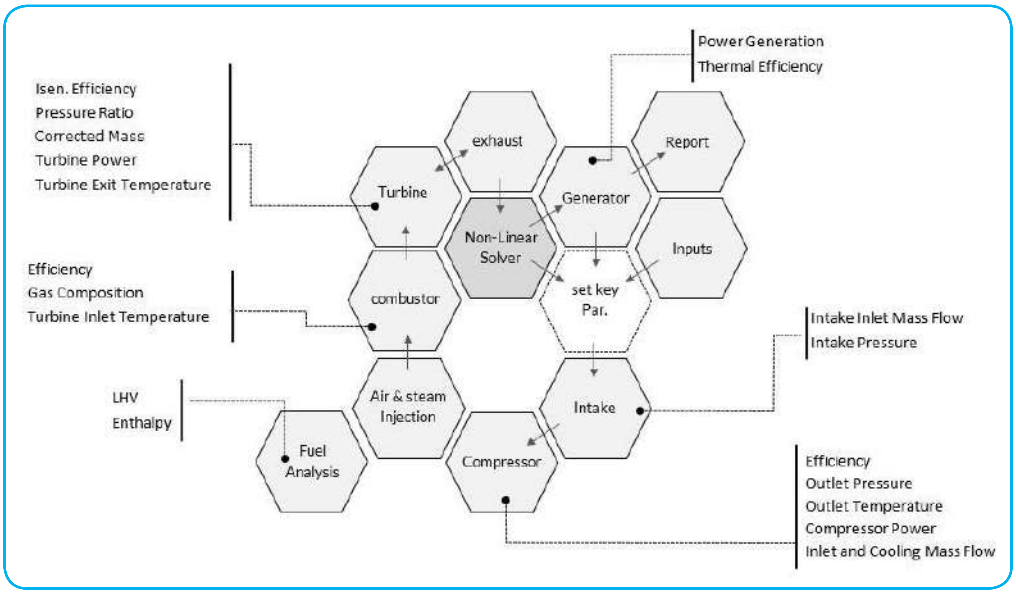

Fig. 2 – MapCycle architecture for performance analysis of a turbogenerator set

This software is used to evaluate performance of different gas turbines of various configurations, including MGT-40 gas turbine, as schematically presented in Fig. 3.

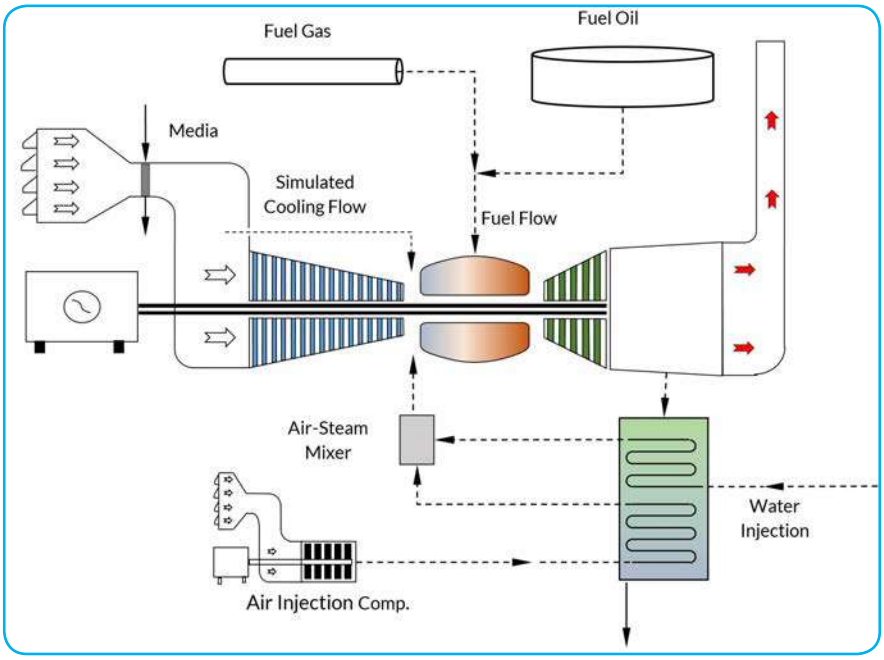

Fig. 3 – Schematic representation of a typical single shaft gas turbine simulated in MapCycle

The results provided by the cycle analysis code are in good agreement with the experimental data, as shown in Fig. 4.

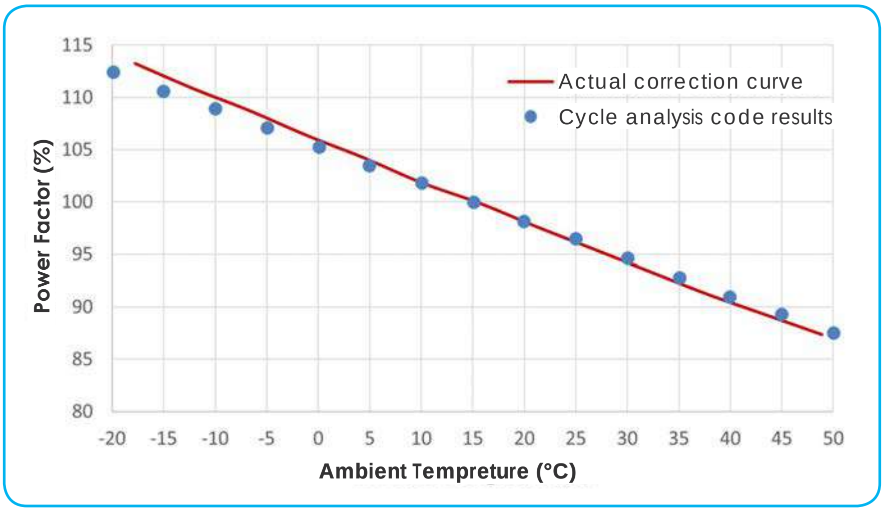

Fig. 4 – Power factor versus ambient temperature for MGT-40 gas turbine

An optimization procedure was utilized to enhance performance of the MGT-40 gas turbine in hot ambient conditions. First, a commercial CFD solver was used to find the impacts of stagger angles on the compressor performance, and subsequently, MapCycle code was utilized to calculate the engine performance.

According to the design of experiment (DoE) analysis results (Taguchi method [3]), engine power at hot ambient conditions is mostly affected by the first five compressor stator vanes. Hence, these five design parameters were considered for optimization purposes. An automatic optimization process based on an internally developed code was used in this study. Genetic algorithms (GAs) and artificial neural networks (ANNs) were coupled with a commercial CFD solver to speed up the process. A flowchart of the applied optimization procedure is depicted in Fig. 5.

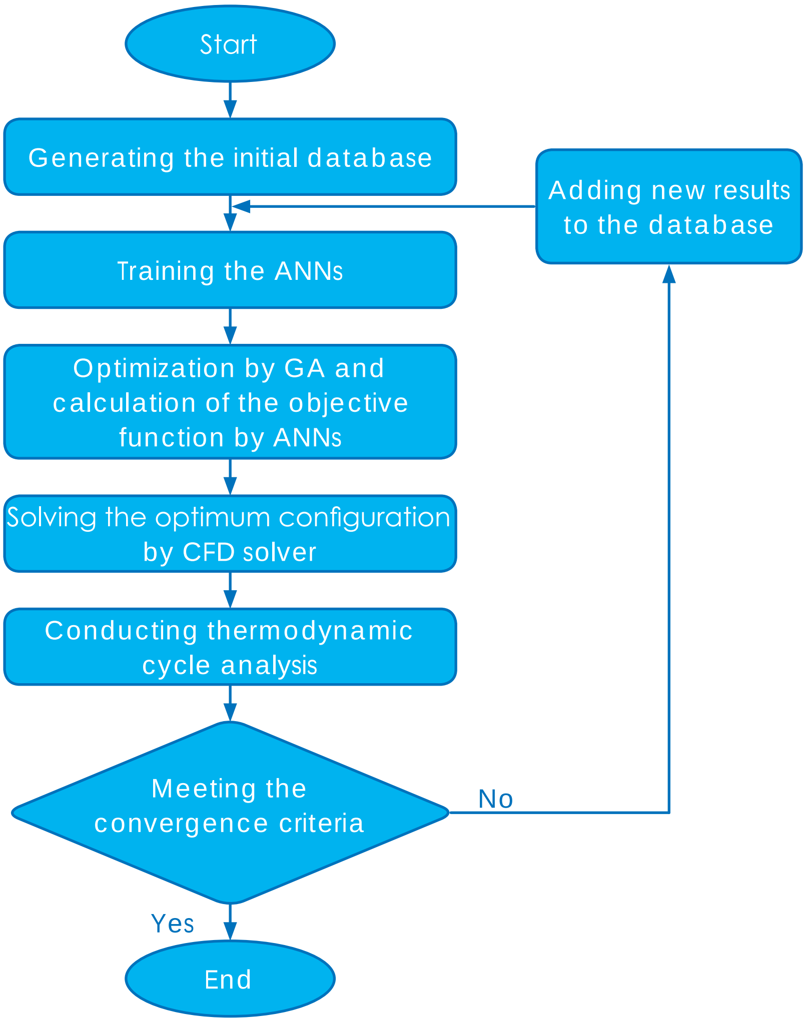

Fig. 5 – Optimization procedure used for MGT-40 gas turbine performance improvement

Direct use of CFD solver leads to a significant increase in calculation time; to reduce this time, ANN was used to predict the engine performance. ANN is made up of several primary processing units called neurons or nodes. The primary purpose of a neural network is to use the information stored in a database to relate design variables of a problem to the corresponding objective functions.

Results & Discussion

Optimal compressor stators' stagger angles contributing to MGT-40 gas turbine performance improvement as the objective function of this study were calculated following implementation of the developed optimization procedure up until the relevant convergence criteria were met.

Compressor maps are presented in Figs. 6 & 7 for original and optimal geometries at various rotational speeds. From these figures it is clear that compressor mass flow rates are noticeably increased in cases of optimum compressor stators' stagger angles at all operating conditions.

MGT-40 gas turbine performance parameters at standard ISO and hot ambient conditions are listed in Table 1 for both the original and optimized compressor blades' geometries. As it is indicated in Table 1, the power output increased by 1.69% and 3.64% at standard ISO and hot ambient conditions respectively.

Table 1 – MGT-40 gas turbine performance parameters

Operating Conditions	Parameter	Original Geometry	Optimum Geometry	Variation
Standard ISO	Power (kW)	40410	41093	683 (+1.69 %)
	Efficiency (%)	30.67	30.59	-0.08 %
Hot Ambient	Power (kW)	33614	34836	1,222 (+3.64%)
	Efficiency (%)	28.81	29.02	+0.21%

Comparison between the results obtained for original and optimal gas turbine compressor blades' geometries clearly indicates that the aim of this investigation, i.e. increasing the MGT-40 gas turbine power output at hot ambient conditions whilst maintaining its power output and cycle efficiency levels at standard ISO conditions, has been achieved.

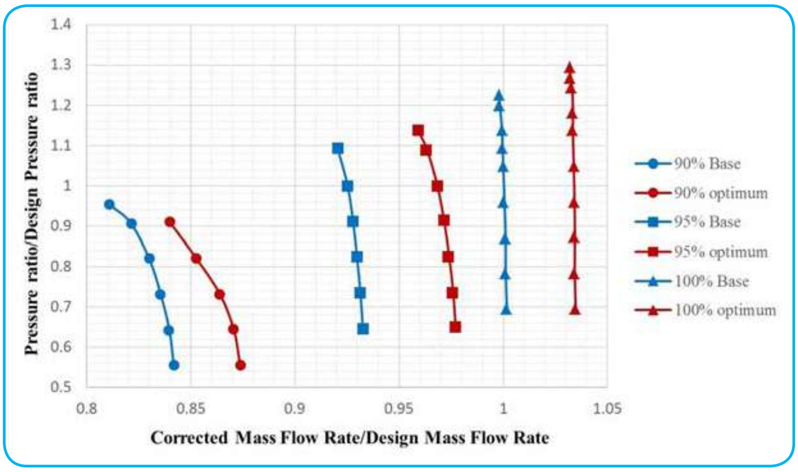

Fig. 6 – MGT-40 gas turbine compressor map for baseline and optimal compressor blades at 90%, 95% and 100% rotational speed

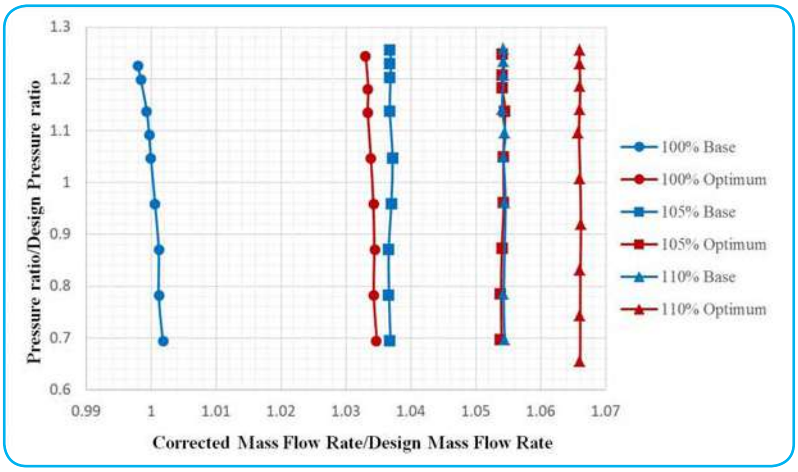

Fig. 7 – MGT-40 gas turbine compressor map for baseline and optimal compressor blades at 100%, 105% and 110% rotational speed

Concluding Remarks

The present work was aimed at improving MGT-40 gas turbine performance at higher ambient temperatures, while maintaining its performance at standard ISO conditions through optimization of stagger angles of gas turbine compressor stator blades. To do so, a variety of tools and software including a commercially available CFD solver, an internally developed cycle analysis code, an evolutionary algorithm coupled with artificial neural networks were utilized. Because of the rather large number of compressor stages, the main challenge for the optimization algorithm to proceed was the high computational time and costs associated with it. So, DoE techniques were utilized to find out which variables significantly impacted the engine performance and it was eventually found that the first five stator blades' stagger angles had the dominant effects on engine power output. Therefore, these five angles were used as design variables in the optimization process. Additionally and due to high computational time associated with the utilized CFD solver, a Genetic Algorithm was coupled with a Neural Network to significantly reduce the time required to calculate the objective function. Eventually, the results indicated that the gas turbine's power output increased by 1.69% and 3.64% at ISO standard and hot ambient temperature conditions, respectively. This was achieved via changing only the first four rows of compressor stators' stagger angles as well as that of the IGV's.

References

[1] M. Ameri, H. Nabati and A. Keshtgar, "Gas turbine power augmentation using fog inlet air-cooling system", *Engineering Systems Design and Analysis: ESDA2004-58101*, PP. 73-78, 2004

[2] A. D. Sa and S. Al Zubaidy, "Gas turbine performance at varying ambient temperature", *Applied Thermal Engineering*, Vol. 31(14-15), PP. 2735-39, 2011

[3] S. D. Bolboacă and L. Jäntschi, "Design of experiments: Useful orthogonal arrays for number of experiments from 4 to 16", *Entropy*, *Vol. 9*, PP. 198-232, 2007

4

Evaluation of Residual Distortions through Simulation of Scan Patterns & Supports for Inconel 625 Additive Manufacturing Process

Fathi, Alborz
Ghodsi, Mahsa
Davarzani, Hossein

MAPNA Turbine Engineering & Manufacturing Co. (TUGA)

Introduction

Selective Laser Melting (SLM) is an additive manufacturing (AM) technique during which high-power-density laser is used to form consecutive metal layers on top of each other by melting and fusing a metallic powder bed according to a predefined model. Since each layer is gradually cooled before the formation of the next, the component, not cooled homogenously, is subject to local heat input and severe thermal gradients causing residual deformations/distortions in addition to stresses which can render the final AM part unfit for use.

Local melt pool geometry, scanning strategy, and part geometry are some of the contributing factors to the extent of residual macroscopic distortions in additively manufactured parts. While the melt pool geometry and scanning strategy (including laser speed, path/pattern, hatch spacing and strip width) mainly affect the local microstructures and anisotropy of the resulting distortions as well, the part and support geometries as well as building orientation play vital roles in the build-up of macroscopic residual distortions/stresses in additively manufactured parts [1].

The complex nature of the SLM method and a plethora of contributing parameters affecting design and manufacturing processes of the parts have prompted the designers to take advantage of the available CAE and FEA tools to identify potential failure modes, eradicating the need for numerous trial and error attempts and allowing for prior adjustment of the parts' geometries and machine parameters to minimize the risk of costly printing errors.

There are many parameters to be considered to achieve an acceptable work piece during the SLM process. In the second article of MAPNA Turbine's Technical Review No.16, the authors determined the effects of heat density on uniformity of the work piece surfaces, amount of residual stresses, dimensional tolerances, microstructures as well as size and shape of defects. It was also mentioned that the heat density level is directly impacted by scan strategy. Scan strategy describes all the parameters to determine how to move laser point on the powder bed to scan the whole selected area. The scan strategy mainly affects residual stresses as well as roughness of the part's final surfaces [2].

The CAE software packages are needed to be calibrated and validated to be reliable in predicting thermal residual stresses within final additively manufactured parts. The goal of the calibration process is to obtain related correction factors for the deployed CAE software. These correction factors help designers to simulate and evaluate the parts prior to the start of AM processes with more reliability, making it possible to modify the supports and redesign the parts if needed.

The present study focuses on the effects of scan patterns and support geometries on residual stresses and distortions during SLM additive manufacturing process of Inconel 625 metal powder on a NOURA M100P machine with a layer thickness of 30 microns. It also investigates how FE software may be used to predict and obtain more accurate residual distortion and help select suitable support geometries prior to the fabrication of any part utilizing the SLM process.

The SLM machine was used to manufacture several parts with specific dimensions. Two different supports and various scan strategies were adopted, and then the actual and numerical results for strain distortions were compared. Correction factors with different scan patterns or scan strategies were obtained. Finally, to confirm and validate the FE coefficients and the suitability of the scan pattern, the numerical and actual results were re-evaluated for a selected group of parts with optimized support.

Simulation Process & Parts Manufacturing

Simulating the build process may be performed at various points along the overall design/manufacturing process depending on the goals pursued. FE software generates solutions to residual stress, distortion, and building failure issues, hence enabling the user to improve the product design, and to inform and validate the build preparation. The overall workflow of the steps taken to attain final distortion values in the present study is shown in Fig. 1.

STEP 1	STEP 2	STEP 3
Manufacturing the part with SLM machine and measuring the distortions	Simulating the manufacturing process and obtaining the distortions via simulation results	Calculating the new SSF and (ASCs) and obtaining the scan pattern and thermal strain analysis results for support optimization
• Models are designed with primary support • The Scan Pattern is determined • Models are built on the platform • Distortions are measured before supports' cut-off • Distortions are measured after supports' cut-off	• Assumed strain and scan pattern simulations are run for primary support • Machine parameters are set • Linear Elastic stress mode is set • Strain Scaling Factor (SSF) is set • Distortions are obtained for the required points and directional component	• Corrected SSF is calculated • Scan pattern simulation is run with corrected SSF and new ASC is found • Support's design is optimized based on simulation results • Simulation distortions are compared with recorded measurements

STEP 4

- Corrected SSF and ASC factors are set and validation analysis is run for the design with new support
- Simulation results are compared with control sample measurements and the simulation error is calculated

Fig. 1 – Overall process workflow of the steps taken to attain final distortion values in this study

1st Step: Manufacturing the Parts with SLM Machine & Measuring the Actual Distortions

■ Models Designed with the Primary Support

For convenience and to maintain the same manufacturing conditions, all parts were built on the same building platform with the same process parameters optimized using the method described in the second article of MAPNA Turbine Technical Review No.16 [2]. All simulation and manufacturing steps were performed on the same cantilever beam model with only scanning strategies and supports (primary and new design) varied. 3-D representations of the cantilever beam model and the holding supports are shown in Fig. 2.

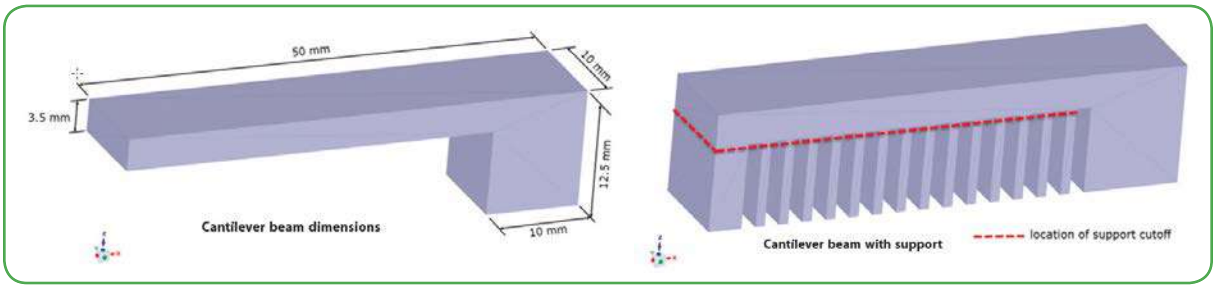

Fig. 2 – Primary model and the holding supports used for simulation and manufacturing purposes

All parts were printed using a NOURA M100P SLM machine in an inert argon atmosphere using Inconel 625 powder with a layer thickness of 30 µm and with two types of support structures directly mounted on the base plate (Stainless steel 316L, 25 cm in diameter and 4 cm high).

■ Design & Determination of Scan Patterns

The CAD model and the STL file were prepared for manufacturing. In the slicing software, primary supports were designed and the scan strategies as well as the hatch spaces were specified.

There are several standard machine parameters, also known as process parameters, used in additive manufacturing simulations. All necessary parameters needed to be determined for scan pattern analysis are listed in Table 1. Each simulation (except the assumed strain simulation) uses some of or all these parameters.

Table 1 – Specifications of different scan patterns used with the manufactures parts

Scan Pattern Strategy	Scan Direction	Starting Angle	Layer Rotation Angle	Hatch feature	Model with Primary support
Scan Pattern 1	Parallel to X direction	0°	0°	Meander	
Scan Pattern 2	Perpendicular to X direction	90°	0°	Meander	
Scan Pattern 3	Rotating stripe (optional scan pattern)	0°	67°	Meander	
Scan Pattern 4	TUGA typical	17°	37°	Chess-board	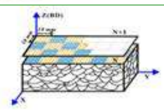

■ Building the Model with Primary Support on the Platform

After modeling and determining the manufacturing strategies, supports were designed for each model. The .CLI files were also created with the slicing software for SLM Machine, and finally the samples were manufactured accordingly, as shown in Fig. 3.

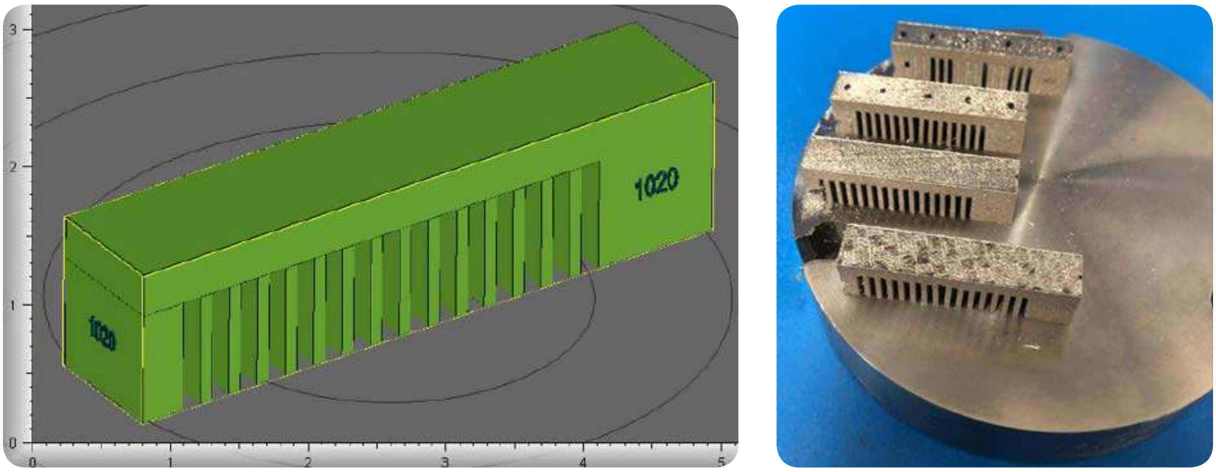

Fig. 3 – Designed part with the primary supports (left);
built models using the SLM machine (right)

■ Measurements of distortions prior and after cutting off the supports

For quantitative characterization of residual distortions after printing according to the proposed instructions, the parts were meticulously measured using digital gauges in two instances of before and after cutting off the supports from the building platform.

The measurement paths for each of the mentioned cases are shown schematically in Fig. 4.

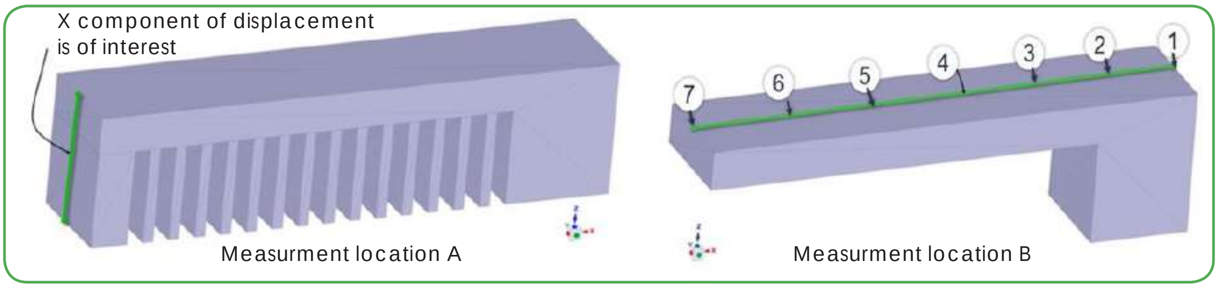

Fig. 4 – Schematic representation of measurement paths A & B

The line charts of actual distortion values measured along path B of the additively manufactured parts are plotted in Fig. 5. According to the results, scan patterns 3 & 4 yielded nearly the same results and so the maximum distortion values belonging to the scan pattern No. 4, i.e. chessboard, was considered and presented in Fig. 5.

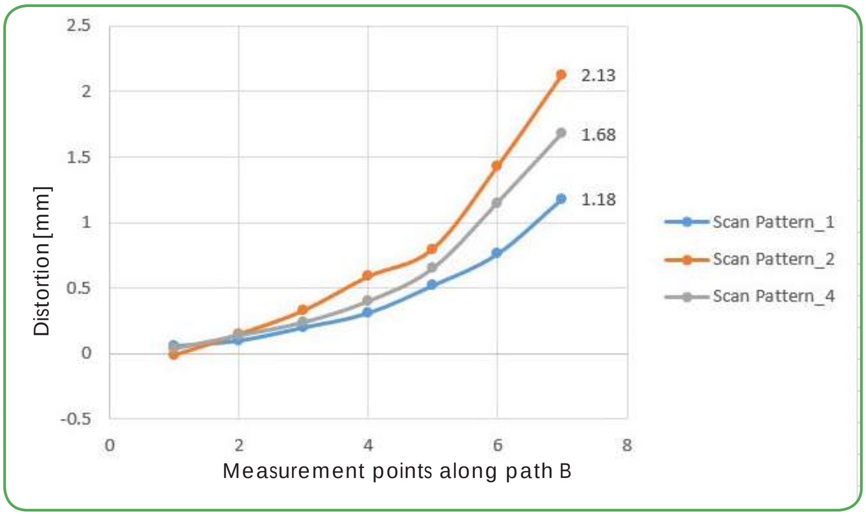

Fig. 5 – Actual distortion values measured along path B for different AM parts manufactured with different scan patterns following cutting off the supports

2nd Step: Simulation of the Manufacturing Process

The objective of the second step was to determine the Strain Scaling Factor (SSF) and Anisotropic Strain Coefficients (ASCs) for thermal strain analysis calculations. The calibrated SSF and ASCs will significantly improve the prediction accuracy of the simulation software, and hence the chance of successful builds along with reducing the cost of trial-and-error experiments. In this study, a purely elastic model was used to achieve a more accurate prediction in the residual stress level as well as the associated residual deformation. The values for SSF and ASCs depend on the following parameters:

- Material
- SLM machine used
- Machine parameters including laser power, scan speed, layer thickness, base plate temperature, hatch spacing, slicing strip width, scan pattern, etc.
- Simulation type performed (assumed strain, scan pattern, or thermal strain)
- Selected stress mode (linear elastic or elastic-plastic)

■ Assumed Strain (AS) Method

Assumed strain (AS) analysis is the simplest and fastest simulation type. It assumes a constant, isotropic strain at every location within a part as it is being built. Anisotropic effects or process dependencies are not directly considered and AS relies solely on material and machine-specific calibrations of the isotropic SSF. Neither process nor scan strategy parameters are required for this simulation type.

SSF is an important factor quantifying the variables specific to each build scenario. It must be experimentally determined for each combination of machine/material/strain/stress mode.

■ Scan Pattern (SP) Method

The scan pattern (SP) mode uses the same strain as the assumed uniform strain, but it takes the scanning direction into account, as well. Larger distortions occur along the laser scanning path than the perpendicular direction. Unlike isotropic distortions in which only SSF needs to be calibrated, in anisotropic distortions, calibration of ASCs is also necessary.

For each scan pattern, the following equations were used to achieve new SSF and ASCs factors which are dependent on the scanning direction.

$$SSF_{new} = \frac{\delta e_{Par} + \delta e_{ver}}{\delta s_{Par} + \delta s_{ver}} SSF_{old} \qquad (1)$$

$$ASC_{Par} = \frac{2}{(1 + \frac{\delta e_{ver}}{\delta e_{Par}})} \quad ASC_{ver} = 2 - ASC_{Par} \qquad (2)$$

Where:

ASC stands for anisotropic strain coefficient

δe_{Par} means parallel to the scan direction and

δe_{ver} means perpendicular to the scan direction

- **Thermal Strain (TS) Method**

The thermal strain (TS) simulation type is the most accurate approach as thermal ratcheting effects and inhomogeneous cooling are taken into account. Since this method requires a thermal prediction for every scan vector, a much longer computation time is required. Like the SP approach, both isotropic and anisotropic strain scaling factors need to be calibrated based on the measured data.

In addition to the material and scan strategy parameters, TS approach also requires the actual process and scan strategy parameters like the laser power and speed, base plate temperature and layer thickness as well as hatch spacing and stripe width to be set.

3rd Step: Calculating New SSF & ASCs and Designing a New Support

- **Assumed Strain (AS) Analysis**

Maximum distortion values were recorded once the AS simulations were conducted. Since this approach does not account for anisotropic effects, the predicted width deviations were equal in both X and Y directions. As mentioned before, the AS simulation approach is not dependent on the scan pattern and hence chessboard pattern was used. The simulations were repeated until the errors became less than the allowable limit (<1%).

- **Scan Pattern (SP) Analysis**

Consideration of the anisotropic effects through using this approach improves the prediction for both bidirectional and rotating scan strategies. The maximum distortion values of the cantilever beam and the supports calculated using this analysis method is shown in Fig. 6.

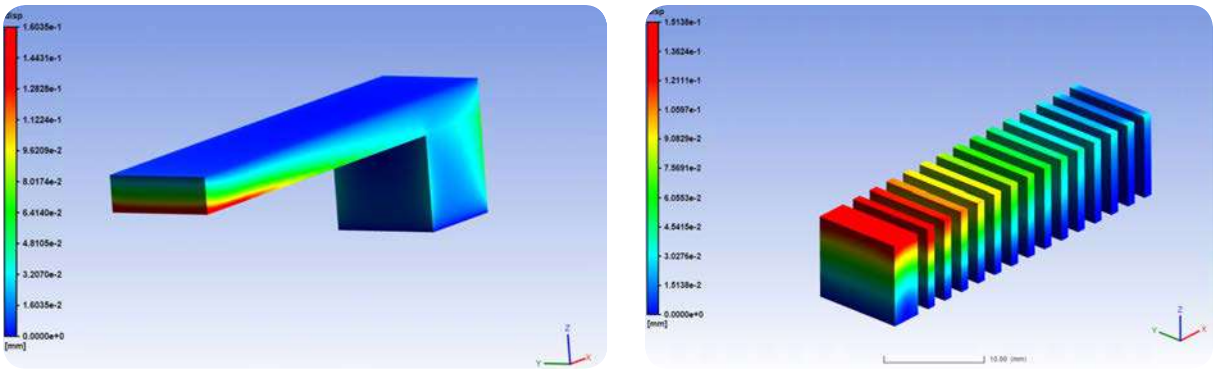

Fig. 6 – Maximum distortion values in the main part (left) and in the supports (right) calculated using the SP simulation method

For both the parallel and orthogonal modes, the preliminary results were extracted. For error rates greater than the allowable limit, i.e. above 1%, the analyses have been repeated till the errors were brought within the acceptable range.

■ Thermal Strain (TS) Analysis

After the scan pattern analysis, the thermal strain analysis using the primary data was conducted. The results for both parallel and orthogonal modes are displayed in Fig. 7. The analyses were again performed using the new data acquired at each step till the errors reached the allowable limit, i.e. below 1%.

SSF and ASCs Calibration for Thermal Strain Simulations

Geometry Measurements	Distortion (mm)
‖ direction (Autofab:90,0-1021)	2.13
⊥ direction (Autofab:0,0-1020)	1.18

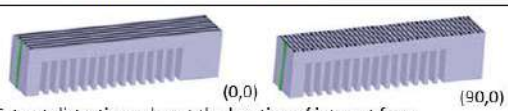

	Simulation iteration	Simulation number		Distortion (mm)	Simulation settings SSF	ASC ‖	ASC ⊥	New settings SSF	ASC ‖	ASC ⊥	Error%
Linear Elastic	1st		‖ direction	3.341	1	1.5	0.5	0.7100	1.2870	0.7130	56.9%
			⊥ direction	1.321							11.9%
	2nd		‖ direction	2.067	0.7100	1.2870	0.7130	0.7102	1.3217	0.6783	3.0%
			⊥ direction	1.242							5.3%
	3rd		‖ direction	2.115	0.7102	1.3217	0.6783	0.7109	1.3314	0.6686	0.7%
			⊥ direction	1.192							1.0%
	4th		‖ direction	2.130	0.7109	1.3314	0.6686	0.7111	1.3309	0.6691	0.0%
			⊥ direction	1.179							0.1%

Fig. 7 – SSF & ASCs calibration for TS simulations

■ Simulation of Residual Deformations & Extraction of Correction Factors

Preliminary results from the first simulations carried out for each type of analyses were recorded and recalculated based on the relationship between the new coefficients and the error rate. For error rates greater than 1%, the simulation process had to be repeated with the latest acquired data. The final results of the analyses carried out to obtain the SSF parameter, as well as ASCs at different modes are summarized in Table 2.

Table 2 – Final results obtained for SSF & ASCs following conclusion of all analysis schemes

Summary of Results							
Material	**Stress Mode**	**Assumed Strain**		**Scan Pattern**		**Thermal Strain**	
Inc625	Linear Elastic	SSF	0.93	SSF	1.5	SSF	0.711
				ASC ‖	1.29	ASC ‖	1.331
				ASC ⊥	0.71	ASC ⊥	0.669
				ASC_z	1	ASC_z	1

Results of the TS simulations performed for calculation of the maximum distortion utilizing the data specified in Table 2 indicate 0.0004 and 1.671 mm distortion values for the beam and supports respectively prior to and after removal of the supports, as shown in Fig. 8.

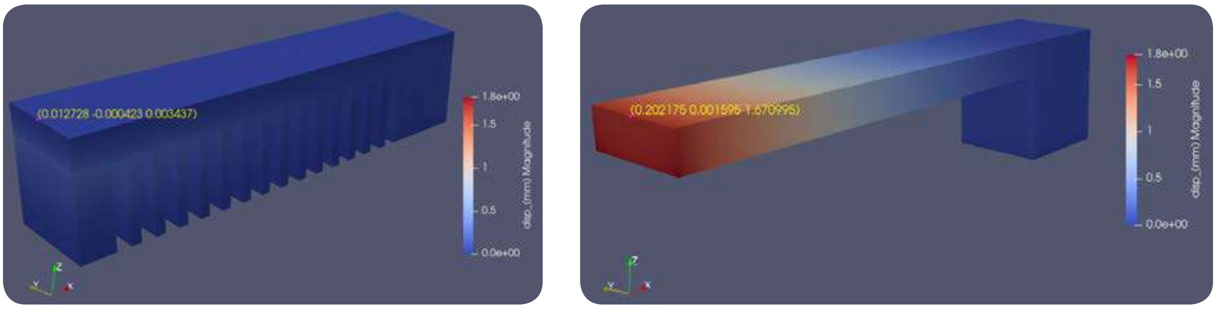

Fig. 8 – Maximum distortions obtained by TS simulations prior (left) and after (right) removal of the supports

■ Designing a New Support

To reduce the maximum distortion encountered, a new support was designed based on the primary simulation results from the TS analysis. More supports with less distance between them were put in place. Once all the simulations and AM process of the new parts concluded, the results were obtained and compared to each other. An integrated model of the part and supports as well as associated AM built models are shown in Fig. 9.

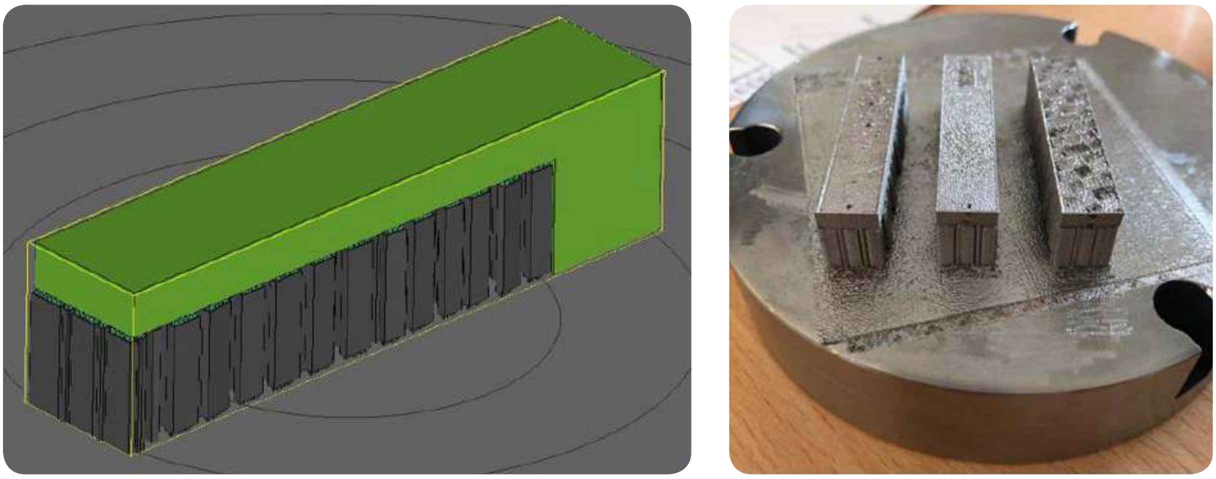

Fig. 9 – Designed part with newly developed supports (left); built models using the SLM machine (right)

4th Step: Validation of Calibration Factors with the New Support

■ Residual Deformations

In order to confirm the results, other tests were also performed on the same AM part using the newly developed support. The dimensions of the part and initial settings - except for the manufacturing strategy which was chosen to be of the chessboard pattern with changing angles in each layer as well as the rotation angle - were all kept unchanged.

The line chart of actual distortions measured at the specified points previously indicated along the AM parts are plotted in Fig. 10. The maximum actual distortion measured to be 1.48 mm in the case of scan pattern No. 4 which yielded acceptable results in terms of mechanical properties.

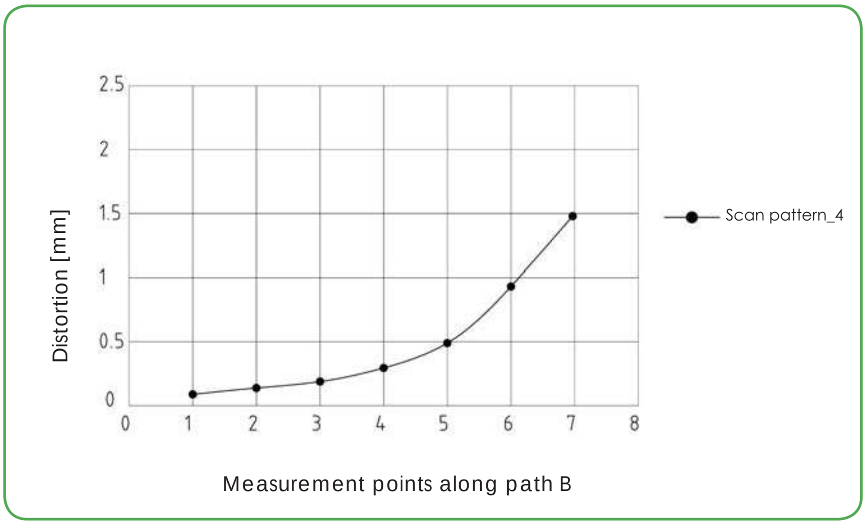

Fig. 10 – Actual distortion values measured along path B of the AM part manufactured with scan pattern No.4 following cutting off the new supports

■ **Validation of Calibration Factors With Newly Developed Supports**

Thermal strain analysis was performed for the part with the new support taking advantage of the correction factors listed in Table 2. According to the results of the simulations performed, the maximum distortion values of 0.003 and 1.45 mm were predicted for the beam and supports respectively prior to and after removal of the supports, as shown in Fig. 11.

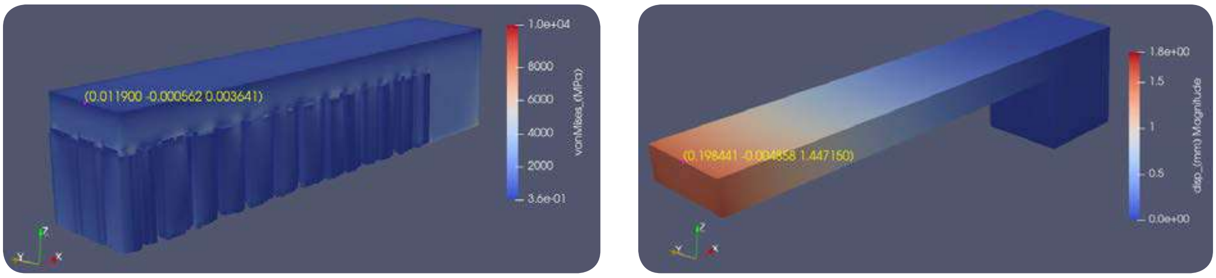

Fig. 11 – Maximum distortions obtained by TS simulations prior (left) and after (right) removal of the new supports

Concluding Remarks

Simulation of the additive manufacturing process plays an important role in the design of AM parts, and is a key to the transition from a mere experience-based to a more knowledge-driven design process that exploits the full potential of this manufacturing technique.

This study was aimed at presenting a fresh insight into the current capabilities of FE software and may serve as a benchmark study for future investigations. The following points should be considered to get a realistic view of the applicability and reliability of the simulation approaches:

- All presented simulation approaches provide reliable predictions of shape deviations in the investigated parts that are within measurement uncertainties of less than 1%.
- According to the results obtained from the calibration, applying the determined correction factors to any other Inconel 625 AM part printed by NOURA M100P can guarantee probability error of less than 1% for residual deformations in FE analysis.

- The final simulation results and measured distortion values subsequent to using newly developed supports show that residual distortion could be reduced by a support that is redesigned based on the simulation data.
- The residual distortion is sensitive to the scan pattern; and chessboard pattern is more suitable than merely longitudinal or transverse scanning schemes.

It is highly recommended to recalculate the correction factors for FE software upon any change in the machine, material or layer thickness. It is also suggested that the same calibration process be performed for different materials (specifically 316L Stainless Steel, Titanium and other Inconel alloys), geometries, support structures, process parameter sets and other machines.

Having the discussed software values also contributes to prediction of the adequacy of the supports, the suitability of the part concerning the platform, and the level of residual stresses on the part before manufacturing. This can significantly reduce the cost and time of the AM process.

Verification and validation test determined that regardless of the support, part model, and scan strategy, if the machine and material are not changed, the simulation results will remain valid with a high probability percentage.

References

[1] T. Mayer, "Simulation and validation of residual deformations in additive manufacturing of metal parts," *Heliyon, Vol.6(5), 2020*

[2] "First MGT-30 Gas Turbine Additively Manufactured Parts set to render conventional manufacturing process of the part obsolete," *MAPNA Turbine Technical Review*, No. 16, Sep. 2021

5

More Streamlined & Efficient MGT-70 Gas Turbine Manufacturing Process

Shiri, Alireza
Mehrali, Hossein

MAPNA Turbine Engineering & Manufacturing Co. (TUGA)

Introduction

Continuous development and looking for new solutions in bringing more efficiency into our production lines have always been given a top priority at MAPNA Turbine.

MGT-70; our flagship gas turbine, has been in our product portfolio since 2002 and the present article outlines two recent improvements made in its assembly and machining processes.

Eliminating Turbine Dummy Shafts

Traditionally dummy shafts were used for the adjustment of lower casing and hot gas parts as well as to align the turbine and compressor bearings with blade carrier I. Taking novel approaches in the assembly of the MGT-70 gas turbine components such as doing the assembly of the center casing and exhaust casing vertically and not horizontally has rendered turbine dummy shafts obsolete.

This way, casings' diameters are extracted from quality control reports at the conclusion of the machining processes and hence the thickness of the needed shims to fill the gap between the casings can be calculated. By using appropriate shim sizes evenly placed on both sides, the casings will be put in their best aligning positions.

Fig. 1 – MGT-70 gas turbine final assembly processes in progress at MAPNA Turbine workshops

This method is also utilized for all lower casings, so as the corresponding piping runs for the casing I and the pedestal are implemented in the vertical position with much better ergonomic outcomes as well as reduced assembly time.

So, in addition to reaching the mentioned goal of eliminating turbine dummy shafts, some machining operations and dimensions were also changed. For instance, the diameter of the hot gas drain hole was decreased by more than 15 mm.

Elimination of the Second Step of Rotor Blades Grinding Process

Grinding of the MGT-70 gas turbine blade tips was traditionally carried out via a two-step procedure. In the first step, blade tips were roughly ground and the rotor was then installed within the casings. Radial gaps were then measured following tightening of the casings' bolts and final grinding totals required were calculated. The gas turbine was then disassembled in the second step to bring out the rotor to carry out the final blade tip dressing. The finished rotor was once again installed in place and the gaps were checked to verify the blade tip gaps in a trial and error procedure.

So, a careful analysis was performed in an effort to eliminate the second step grinding of the rotor blades and to do it all at once via a single-step procedure.

Initial assessments of the procedure represented more stable and uniform grinding values for compressor blades in comparison with gas turbine blades and hence brought about different treatment of each.

■ Compressor Blades

Initial grinding values were analyzed for 13 recent gas turbines manufactured to find out an optimum value for each compressor stage. Initial grinding values measured at the 2nd compressor stage are represented in Fig. 2. Excluding the initial grinding value corresponding to the 164th gas turbine unit as an outlier in the provided dataset, would yield an optimum grinding value of 0.2 to 0.3 mm for this stage of the compressor as shown in Fig. 3.

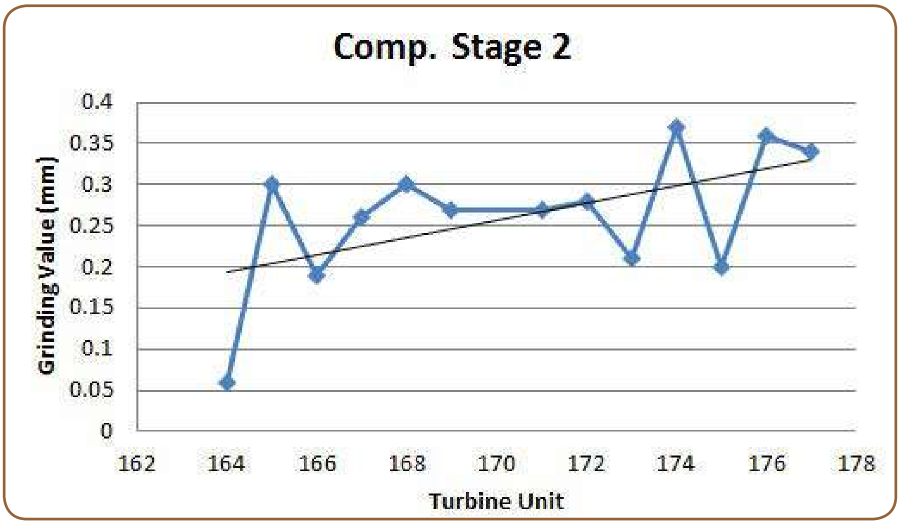

Fig. 2 – Initial grinding values at the 2nd compressor stage of the MGT-70 gas turbine; units 164-177

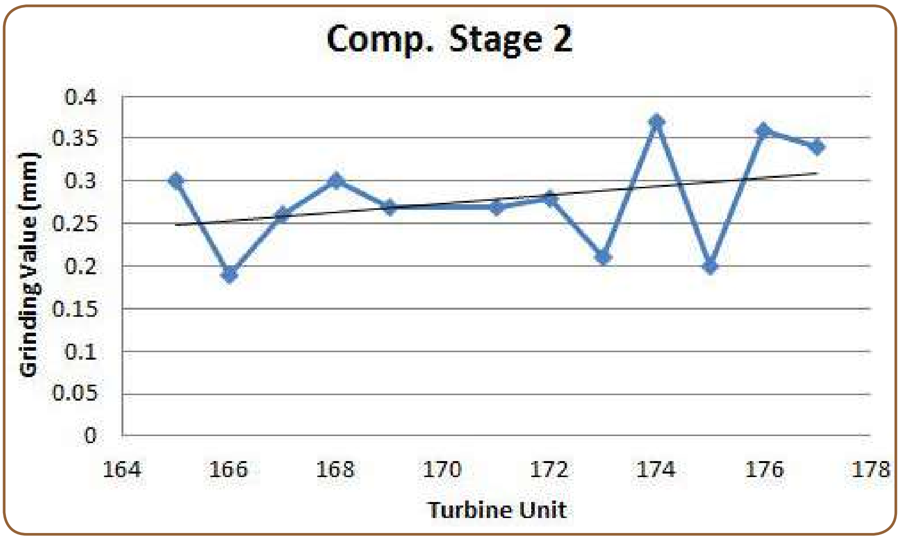

Fig. 3 – Initial & optimum grinding values at the 2nd compressor stage of the MGT-70 gas turbine; units 165-177

In the next step, 0.25 mm final grinding value was theoretically considered for several gas turbines deemed critical (units ground with values far from the mentioned optimum value) to calculate final resulting gaps. Final gaps calculated for the 3 critical units are listed in Table 1. According to the results, applying final grinding value of 0.25 mm for the 2nd stage compressor blades would have resulted in acceptable final gap values in 12 of the 13 cases investigated. Measured gap values at just 3 points of the rotor belonging to the 164th gas turbine unit exceeded the acceptable range by less than 0.1 mm (marked in red color in Table 1).

Table 1 – Critical cases gap measurement data

Critical Units (Grinding 0.25mm) Nominal Gap: 1.8-2.2 mm						
U164	**Gap Real**					
	U	L	UL	LR	LL	UR
	2.13	2.06	2.09	1.93	2.06	1.95
	Gap			IF	grinding	**0.25**
	U	L	UL	LR	LL	UR
	2.32	2.25	2.28	2.12	2.25	2.14
U174	**Gap Real**					
	U	L	UL	LR	LL	UR
	2.12	2.19	2.09	2.1	2.1	2.06
	Gap			IF	grinding	**0.25**
	U	L	UL	LR	LL	UR
	2	2.07	1.97	1.98	1.98	1.94
U176	**Gap Real**					
	U	L	UL	LR	LL	UR
	2.09	2.15	2.02	2	1.98	2
	Gap			IF	grinding	**0.25**
	U	L	UL	LR	LL	UR
	1.98	2.04	1.91	1.89	1.87	1.89

The same approach was applied on all 16 compressor stages to find out optimum grinding values for each stage. For the 182nd gas turbine unit, 50% of the predicted grinding values were applied on compressor blades and these values were corrected following final gap measurements (other parameters such as the over speed test precedence could have impacted these values).

For the next gas turbine, 70% of the corrected values were applied on compressor blades and finally for the 185th gas turbine unit, the predicted values were applied completely and final gap measurements revealed that all gap values were acceptable, as shown typically in Fig. 4, for the first stage compressor blades.

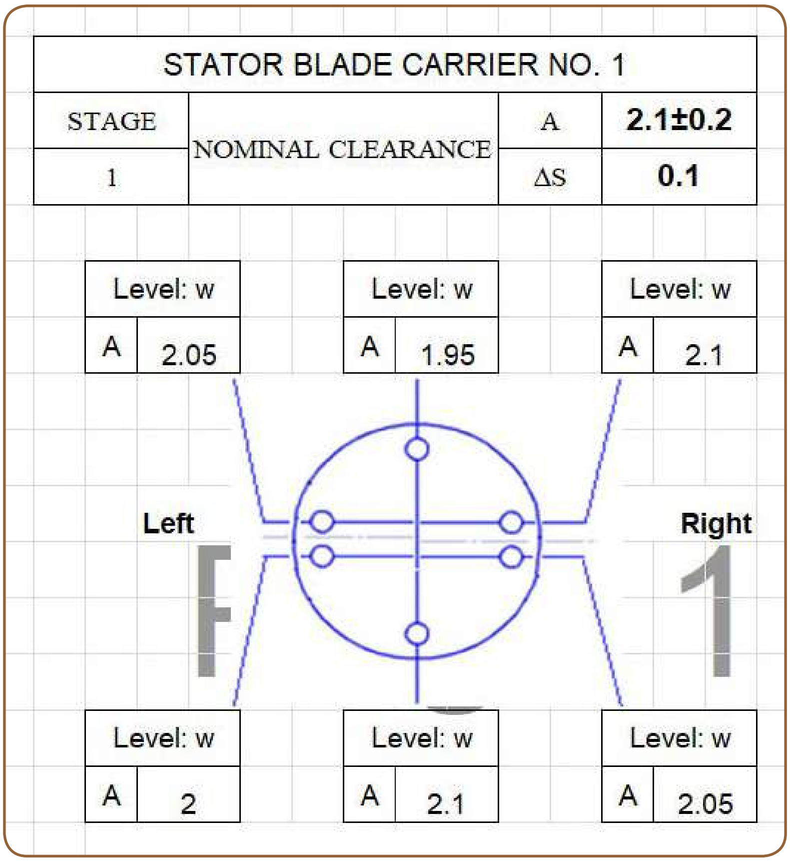

Fig. 4 – First stage compressor blades gap measurement data

■ Turbine Blades

Initial investigation of the grinding values applied at the turbine side revealed that the variations at several blade rows were more than radial gaps' tolerances, as shown in Fig. 5.

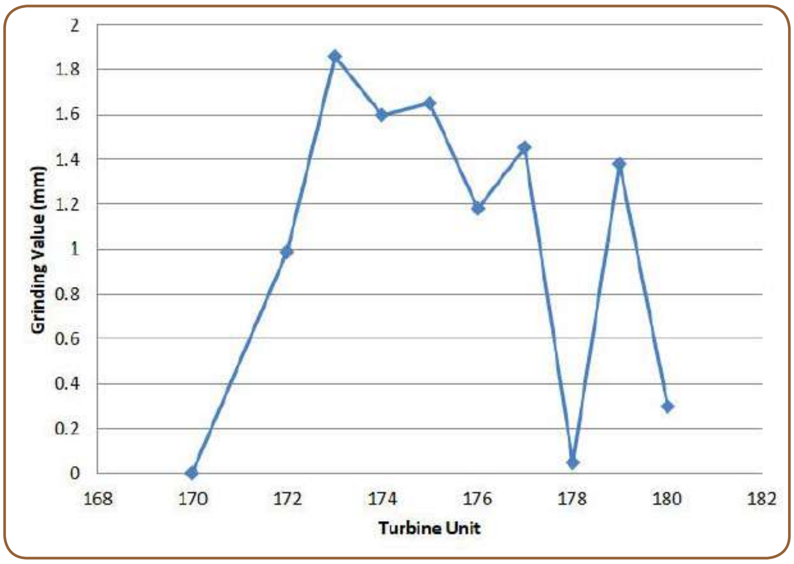

Fig. 5 – Measured grinding values at the 4th stage of the MGT-70 gas turbine; units 170-180

So, it seemed highly risky to determine an appropriate fixed grinding value for each gas turbine stage and hence the two following approaches were taken:

- **Direct Measurement of Rotor & Stator Diameters**

Theoretically, gap values can be calculated when the diameter of male (rotor) and female (stator) pieces are measured. To do so, it is necessary to find out the exact axial position of the rotor inside the turbine carrier, as represented in Figs. 6&7, so the axial locations for measuring gaps on the stator part could be determined.

This was carried out for the 182nd gas turbine unit and the theoretical results obtained showed a quite acceptable conformity with the actual gap measurements carried out.

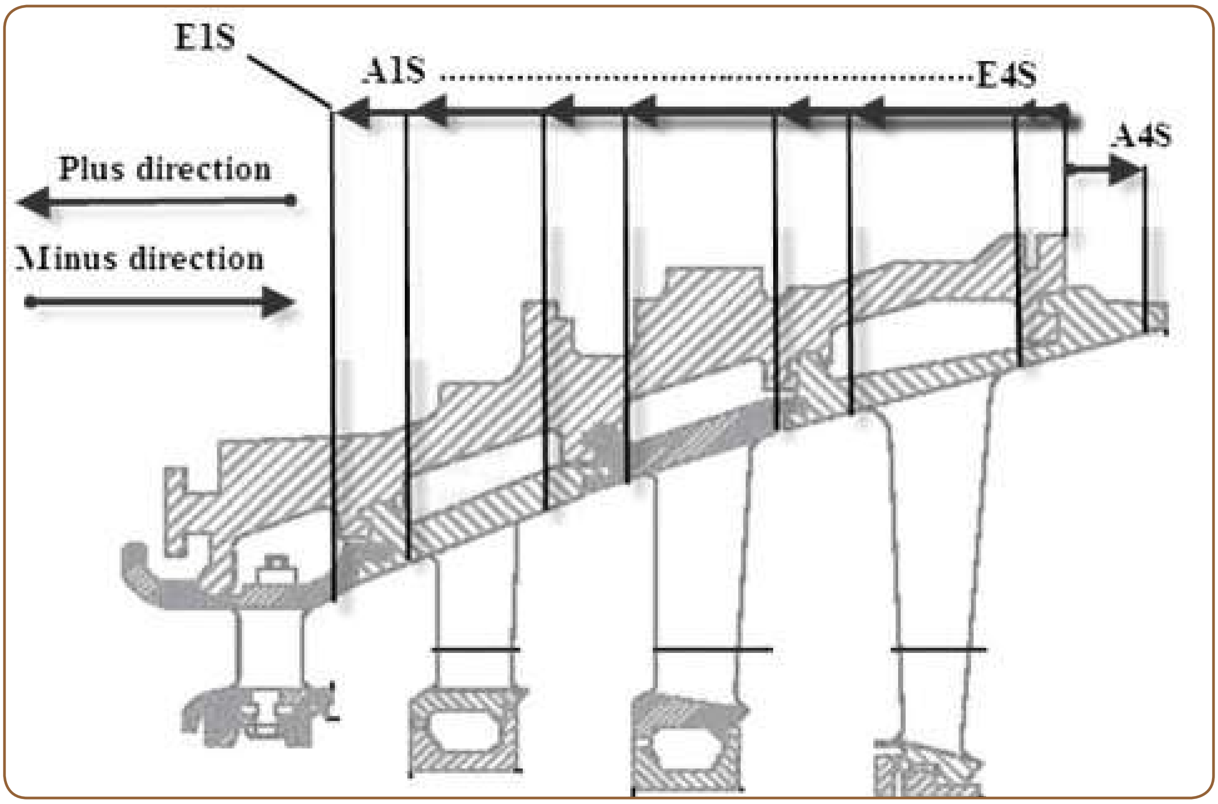

Fig. 6 – Pinpointing the axial position of the stator diameter on the MGT-70 gas turbine blade carrier

The unit order number								G178-40000B
Position		Part name	Design Group	QAG Number	Nominal	Tol.	Actual	Order Number
Center line		Bearing housing Comp.	41105	_	476.00		_	
A		Stator 1, Comp	42210	TR01-42210-001	1509	±0.5	1509.01	G178-42210
A		Center casing	42135	TR01-42135-001	5200	±0.5	5200.10	G177-42135
L3					523	±0.1	522.95	
Z					8	0.2	8.07	
M					75	-0.15/-0.1	74.87	
Shim thickness				_	_	_	15.00	
B		Stator Turbine	12230	TR01-12230-001	535	±0.2	534.96	GA08-12230
C					110	H7	110.02	
							7225.35	
							Z(Axial position)	
D		Rotor	44000	TR01-44000-002	350	0/+0.057	350.03	G178-44000B
St1	Es				_	_	6093.00	
	As				_	_	6164.00	
St2	Es				_	_	6371.00	
	As				_	_	6420.00	
St3	Es				_	_	6653.00	
	As				_	_	6720.00	
St4	Es				_	_	7045.00	
	As				_	_	7146.00	

Axial distance for taking measurment turbine blade carrier diameters									
Position		Axial distance	Diameter		Position		Axial distance	Diameter	
			Min	Max				Min	Max
St1	Es	957.33			St3	Es	397.33		
	As	886.33				As	330.33		
St2	Es	679.33			St4	Es	5.33		
	As	630.33				As	-95.67		

Fig. 7 – Calculations performed for determination of the axial position of the stator diameter on the MGT-70 gas turbine blade carrier

Although application of such a method yielded quite acceptable results, there are still some difficulties as mentioned below:

- Setting the turbine carrier on the measuring platforms for diameter measurement is difficult and highly risky for the carrier part
- Any mistake in finding the exact axial position of measuring points on the turbine carrier would have a significant impact on the obtained results. A negligible mistake of 1 mm in the estimation of the exact axial position would lead to a 0.6 mm change in the measured diameter.
- While doing measurements, the stator is measured and once calculations are finalized, the rotor should be ground simultaneously. Planning and synchronizing these activities are quite difficult as a routine manufacturing program.

Therefore, a second approach was taken to eliminate gas turbine second step grinding procedure in the turbine side, as mentioned below:

► **Assembly Optimization Combined With Statistical Methods**

Utilizing this method, all parameters with potential significant impacts on variation of gas turbine rotor blades' grinding values were addressed to decrease the amount of observed variations.

One of the most important parameters greatly impacting the grinding value of the turbine side rotor blades of different stages is the axial position of the turbine blade carrier.

To address this issue, a comprehensive study was carried out to install the turbine blade carrier in a fixed position using the shims sized accurately following some careful analyses and calculations.

Other major parameters were also adjusted and dealt with delicately to rule out the second step of rotor blade tip grinding. These parameters are as follows:

- Retrospective analysis of axial clearances in previous gas turbines showed that in 85% of cases, it is possible to move the rotor for about 0.6 mm in the positive direction, resulting to almost 0.2 mm change in the radial gaps at the turbine side
- Review and revision of manufacturing processes of stator blades to have quite fixed final stator diameters
- Analyzing out-of-range gap values which could be acceptable in non-conformed cases and the direction of such non-conformities (plus or minus) for increased maneuverability

Taking into account all of the above, and providing appropriate solutions, grinding values were measured in several gas turbines, as shown in Fig. 8. The predicted values were then calculated and applied in part for the next two subsequent gas turbine rotors being manufactured. Finally, following some fine tuning, the predicted values were applied completely on a gas turbine rotor with acceptable gap values in all directions, as shown typically in Fig. 9, for the 4th stage gas turbine blades.

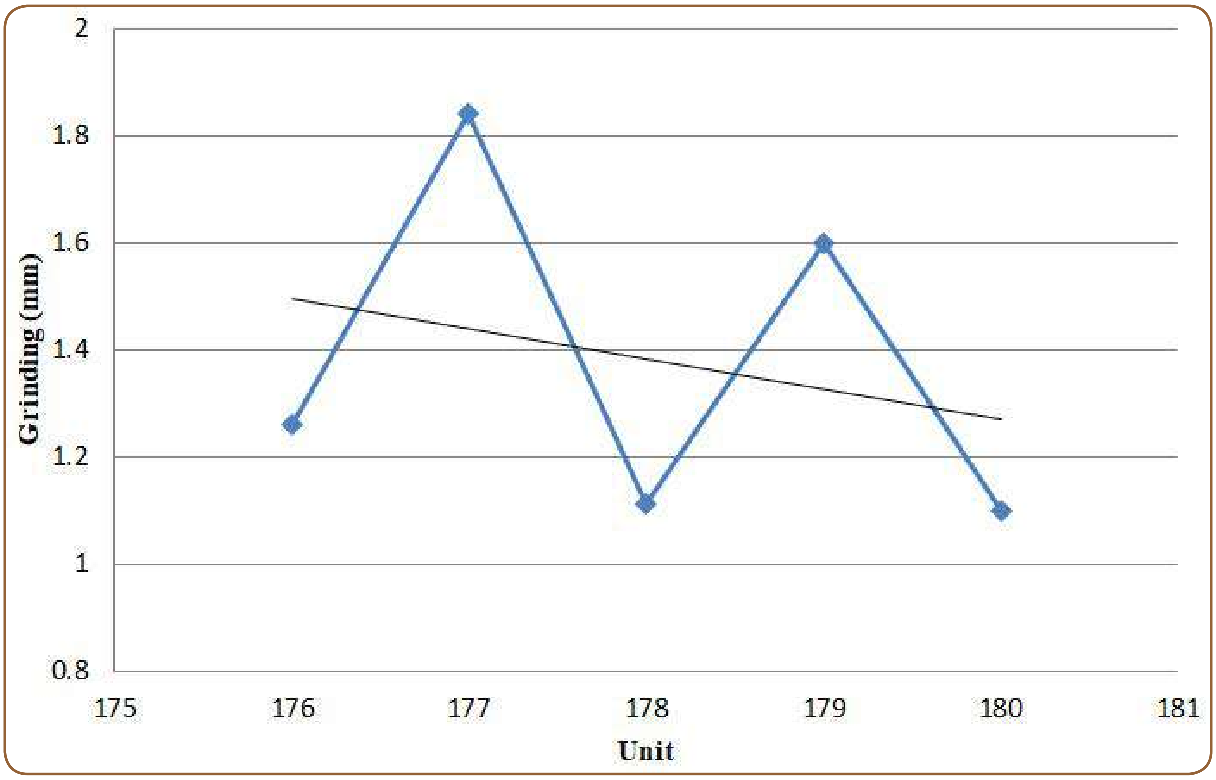

Fig. 8 – Measured & optimum grinding values at the 1st stage of the MGT-70 gas turbine; units 176-180

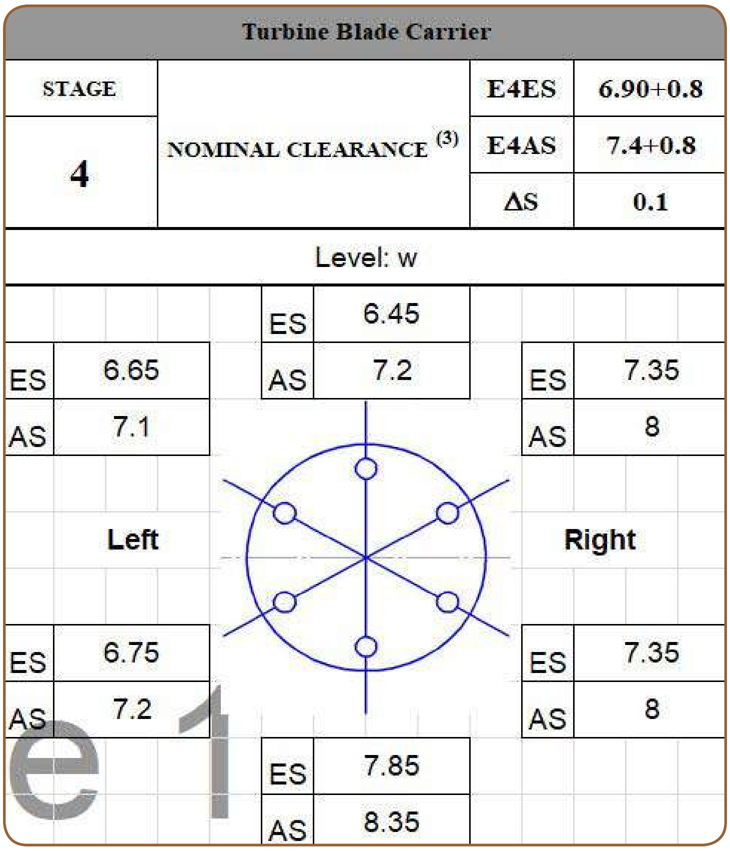

Fig. 9 – 4th stage gas turbine blades gap measurement data; unit 185

The Bottom Line

This article outlined the steps taken to make manufacturing processes of MGT-70 gas turbines more efficient by ruling out and/or optimizing some burdensome and time consuming processes of using dummy shafts for the alignment of different gas turbine components and two-step rotor blade tip grinding procedure. In the course of this project, statistical tools and methods were utilized and several assembly procedure change orders were issued to successfully accomplish the jobs. Consequently, the machining hours and man-hours required for the grinding procedure of the MGT-70 gas turbine rotor were decreased by 50 hrs and 500 hrs, respectively. The critical path of gas turbine final assembly was also reduced by almost 6 working shifts.

Head Office:
231 Mirdamad Ave. Tehran, I.R.Iran.
P.O.Box: 15875-5643
Tel: +98 (21) 22908581
Fax: +98 (21) 22908654

Factory:
Mapna blvd., Fardis, Karaj, I.R.Iran.
Post code: 31676-43594
Tel: +98 (26) 36630010
Fax: +98 (26) 36612734

www.mapnaturbine.com
tr@mapnaturbine.com

GR530-0